fea INFORMATION Engineering Solutions

Ansys LST

Issue 4, April 2021

www.lstc.com www.ansys.com www.feapublications.com

ANSYS

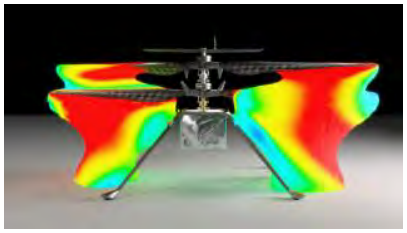

LST

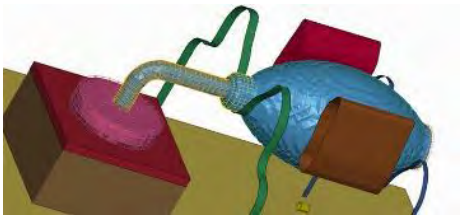

ETA

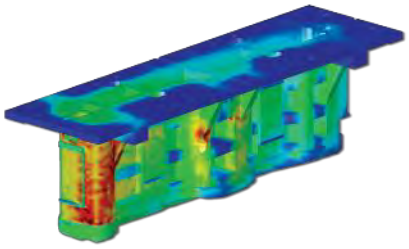

OASYS

LS-DYNA@ New Feature and Application

- **On Setting up a 2D Structured ALE Model**
- **Electrochemical-Thermal-Mechanical coupling of Lithium-Ion Battery Model in LS-DYNA**

FEA Information Engineering Solutions

www.feapublications.com

The focus is engineering technical solutions/information.

Livermore Software Technology, an ANSYS company

Development of LS-DYNA, LS-PrePost, LS-OPT,
LS-TaSC (Topology), Dummy & Barrier models and
Tire models for use in various industries.

www.lstc.com

To sign up for the FEA News send an email - subject "subscribe" to news@feainformation.com
To be removed from the FEA News send an email - subject "Remove" to news@feainformation.com

If you have any questions, suggestions or recommended changes, please contact us.

Editor and Contact: Yanhua Zhao - news@feainformation.com

Platinum Particpants

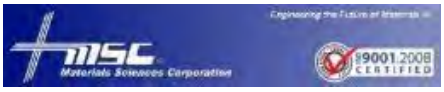

Table of contents

Announcements

LS-TaSC® New Release Version 2021 R1

With the 2021 R1 release, LS-TaSC continues to expedite the optimization design process, enabling complex large nonlinear MDO problems to be tackled efficiently. A summary of top new features in LS-TaSC 2021 R1 is described as below.

Efficiency Improvements for the Multidisciplinary Design Optimization: Following the computation capabilities of the previous release in addressing constrained multidisciplinary topology optimization problems, 2021 R1 aims to improve the computational efficiency in multipoint analysis in the optimization design workflow. Disciplines with analytical design sensitivity information such as NVH load cases will no longer do a full multipoint analysis – the values for the sibling designs will be predicted instead. This enables the function evaluation time for NVH analyses at sibling points to be decreased enormously in each iteration.

Facilitating Various Needs for NVH Design Optimization: The 2021 R1 supports computations using the design sensitivity information in NVH load cases for different design needs, such as a frequency gap "$f_3 - f_2$", and a normalized frequency constraint "$f_2/1000$". This also enables a frequency for a particular design purpose to be used as an objective for NVH design optimization.

Support for Structures using Rubber Materials: The 2021 R1 now supports structural designs for using materials *MAT_MOONEY-RIVLIN_RUBBER, *MAT_HYPERELASTIC_RUBBER, and *MAT_OGDEN_RUBBER.

Minimum Member Size Control: The latest release provides better control of minimum member size for parts, which can be selected from the method panel.

Better Support for Design of Head Injury Criterion: The 2021 R1 now enables to extract and define the HIC (Head Injury Criterion) responses directly from the constraint panel.

Support for STL Outputs: The 2021 R1 now provides the STL outputs of the isosurface plots of the optimized designs. The STL outputs can be used to create CAD version of the optimal designs through third-party tools.

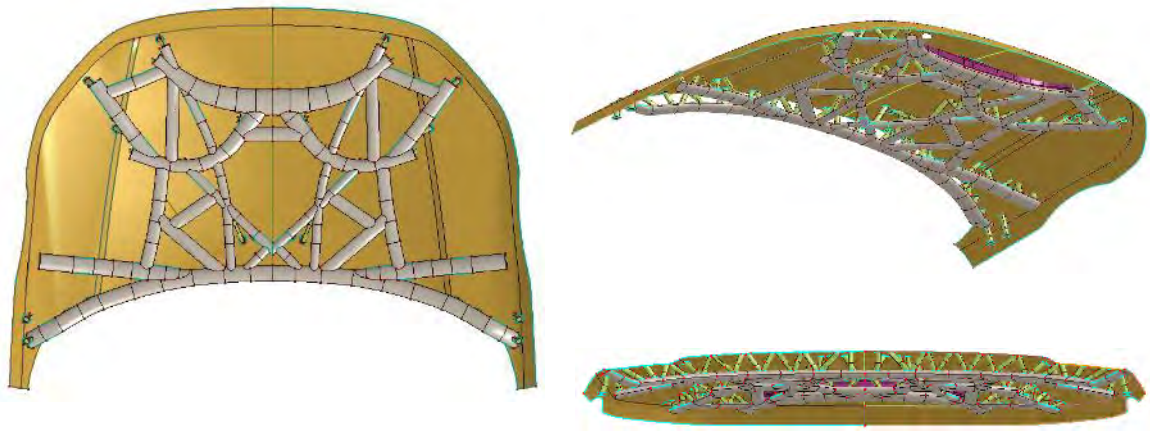

The CAD model of a LS-TaSC hood design as created using ANSA. CAD model courtesy of BETA CAE Systems.

New version download: http://ftp.lstc.com/user/ls-tasc/2021R1_beta/

Ansys

Ansys Blog

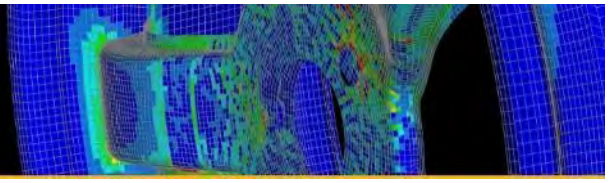

APRIL 8, 2021

How Simulation Is Helping Make History: The First Flight Attempt on Mars

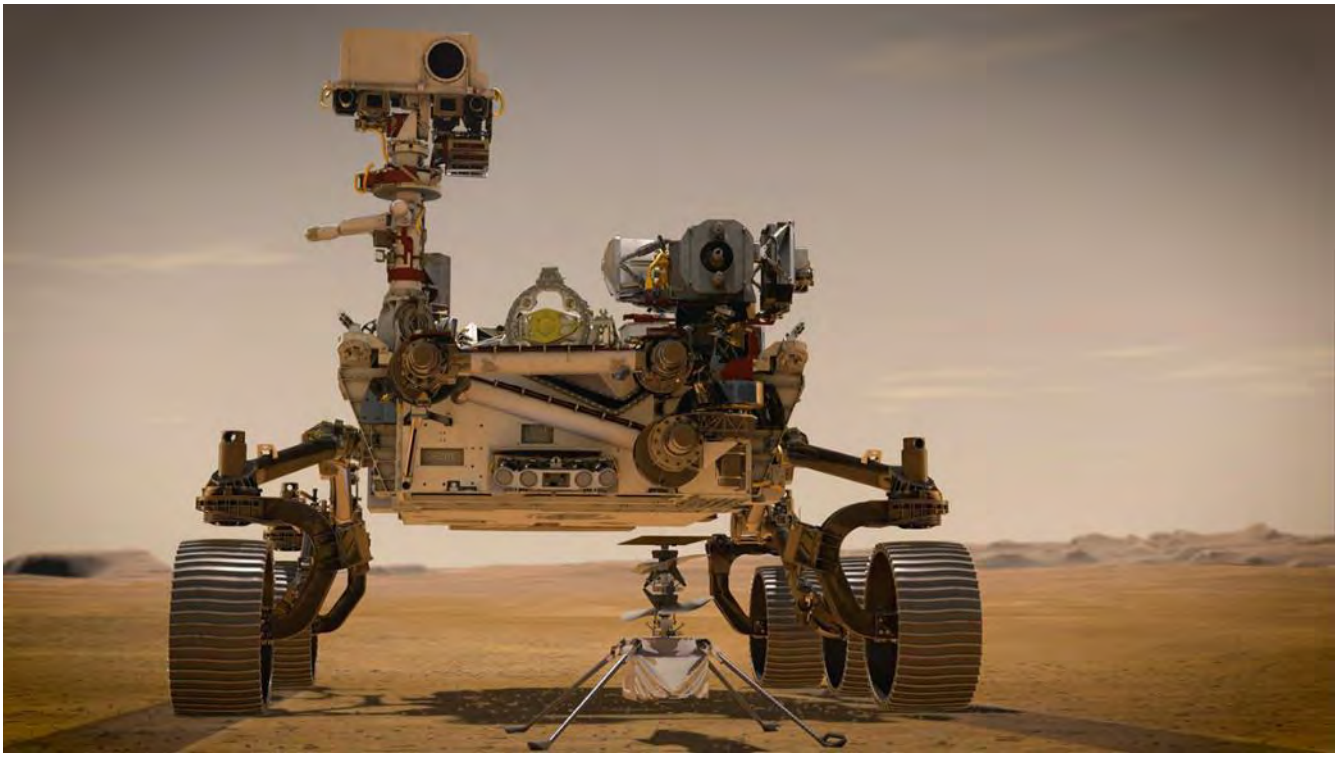

An illustration of the NASA Perseverance rover and Ingenuity helicopter on Mars. Credit: NASA/JPL-Caltech

NASA is making history with a 4-pound (1.8 kg) helicopter named Ingenuity. The world is about to witness an attempt of the first powered flight on another planet.

NASA's Perseverance rover, where Ingenuity was stored, touched down on Martian soil on Feb. 18, 2021. On April 4, the Perseverance rover dropped Ingenuity onto the surface of the Red Planet. NASA plans for the helicopter to take flight along the surface of the Jezero Crater no sooner than April 11 with a series of flights over a 31-day window.

It is difficult to anticipate the potential challenges of flying on Mars. Simulation and wind tunnels are critical to flight tests because they can replicate what an aircraft will experience. Accurate recreation of another planet's gravity and atmosphere on Earth is nearly impossible, so the key to a successful maiden flight will be simulations that are truly out of this world.

The Challenges of Flying on Mars

The main challenge to Mars flight is the very thin atmosphere. The world altitude record for helicopter flight on Earth is held by Frenchman Frédéric North1 at 42,500 feet. The air at that stratospheric level is so thin that North's helicopter rotors could no longer lift him higher. On the surface of Mars, the atmospheric density is equivalent to Earth at 100,000 feet. The Ingenuity helicopter will rely on a light design, large coaxial rotors and the lower Martian gravity to fly in such extreme conditions.

The Martian flight environment is vastly different from Earth's:

- Density 1% of Earth's
- 95% carbon dioxide
- Gravity a third of Earth's
- Average temperature of -60 C (-76 F), with nights as cold as -90 C (-130 F) at Jezero Crater

Once Ingenuity leaves the ground, maintaining directional control in such a thin atmosphere is the big concern. To avoid crashing, continuous corrections are required to rotor pitch, roll and angle of attack on a millisecond-by-millisecond basis. Simulation of the advanced flight control systems is the key to safe flights on Mars, but this requires accurate aerodynamic data.

Flight on Mars may be theoretically possible, but will there be enough control to let it succeed?

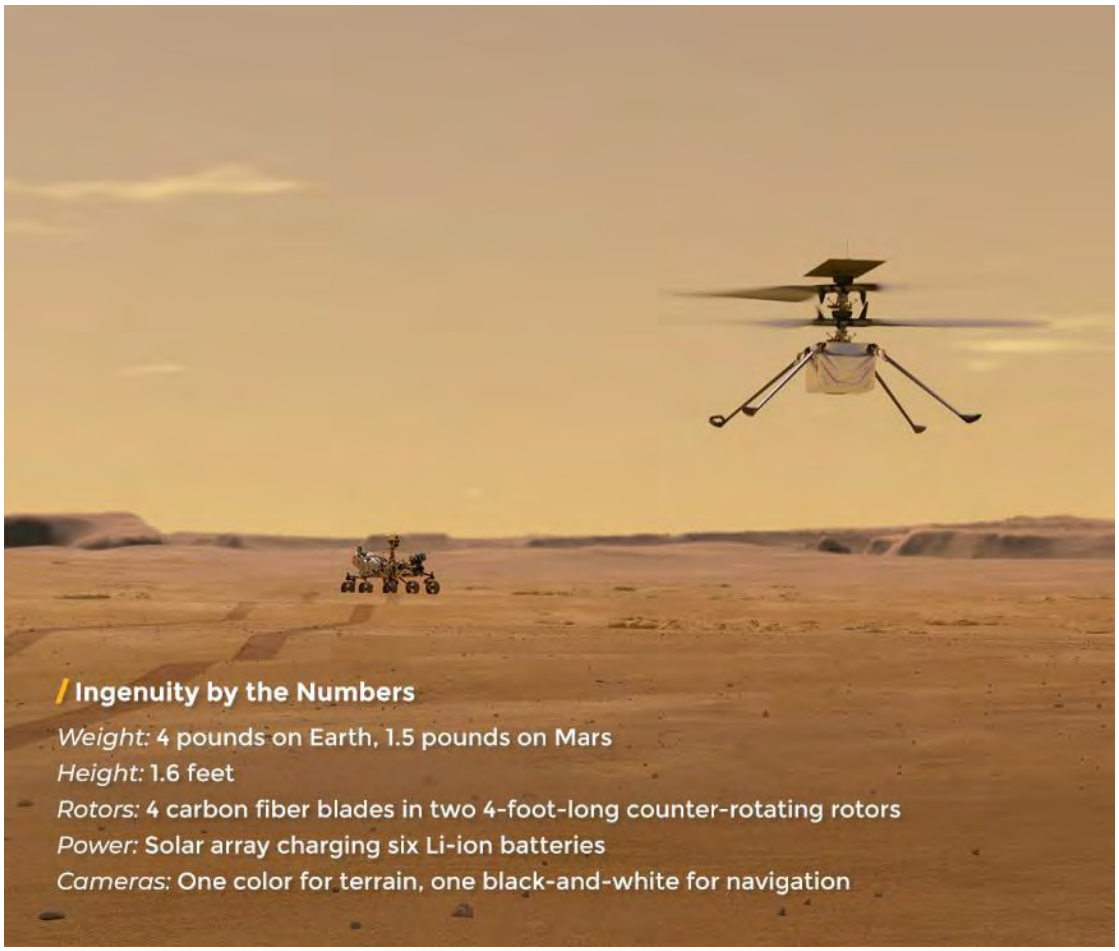

An illustration of NASA's Ingenuity helicopter flying on Mars. Credit: NASA/JPL-Caltech

Making Martian Flight Possible with Ansys Fluent

How could NASA be sure they have a helicopter that is going to make the trek to Mars and have a chance of flying? Ansys Fluent.

According to a research paper2, Fluent was used to calculate the aerodynamic forces on the rotor blade. To predict these forces, the rotor blade was divided into many slices that included span, chord, twist and sweep.

Coefficients of lift, drag and pitch moment as a function of angle of attack and Mach number were then calculated. These values were tabulated and used for helicopter flight dynamics modeling at NASA.

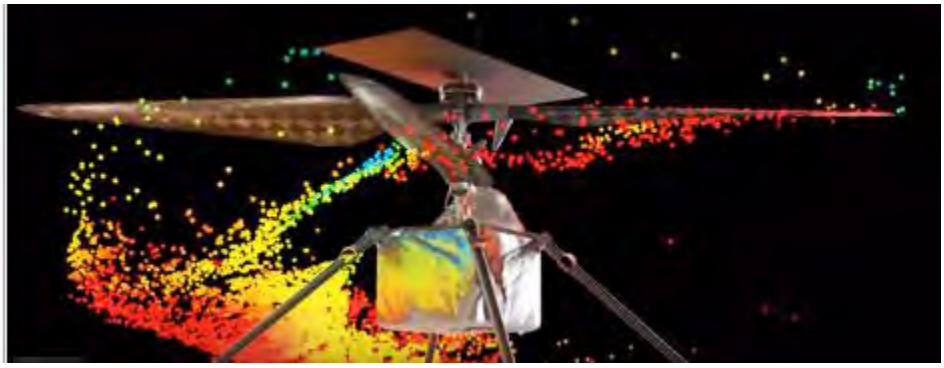

(Go to website to watch the simulation)

The simulation above5 shows massless tracer particles that highlight the impact of the rotors as they slice through the atmosphere. The tracer particles are colored by velocity. We should see maximum velocity (red color) at the rotor and near the tips. We should see lower velocity as the particles make a spiral path to the ground plane. As the rotors pass by one another, we should not see the particles from the lower rotor being pulled up or disturbed by the upper rotor. We want to keep the interaction between the counter-rotating air currents pulled by the rotors to a minimum to ensure maximum lift for the helicopter.

Why not a Quadcopter?

Ingenuity's rotors are arranged co-axially, which is not the popular quadcopter layout of many Earth-bound drones. Why is this?

The main reason for coaxial rotors on Ingenuity is efficiency.

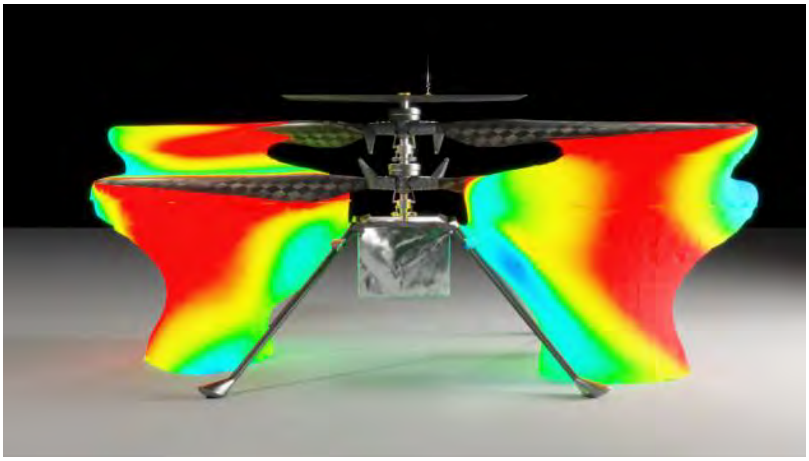

An Ansys simulation showing zones of high pressure under the Ingenuity helicopter rotors.

The image above depicts zones of high pressure under the rotors. Pressure zones under the lower rotor are larger because the upper rotor has already compressed the thin Martian atmosphere. This phenomena allows the lower rotor to provide more lift. A quadcopter, with its four independent rotors, does not have this advantage. Additionally, a quadcopter would be slightly heavier for the amount of thrust produced. Extra rotor supports and multiple motors add weight. Finally, a quadcopter would have difficulty being stowed and then unfolded from the belly of the Perseverance rover.

Records Already Broken

Ingenuity is what is known as a technology demonstration – a project that seeks to test a new capability for the first time, with limited scope, according to NASA. If successful, it will have been the result of more than six years of work by engineers on the Ingenuity team.

They have already demonstrated that it is theoretically possible to build an ultra-lightweight craft that could generate enough lift in Mars' thin atmosphere to take off from the ground, and operate and survive autonomously in the challenging Martian environment. As NASA says: These accomplishments have already pushed the boundaries of flight.

"When NASA's Sojourner rover landed on Mars in 1997, it proved that roving the Red Planet was possible and completely redefined our approach to how we explore Mars. Similarly, we want to learn about the potential Ingenuity has for the future of science research," said Lori Glaze, director of the Planetary Science Division at NASA Headquarters via a press release. "Aptly named, Ingenuity is a technology demonstration that aims to be the first powered flight on another world and, if successful, could further expand our horizons and broaden the scope of what is possible with Mars exploration."

This is an exciting time to watch as simulation and science redefine planetary exploration.

Additional Resources

1. Fred-North.com

2. Flight Dynamics of a Mars Helicopter

3. Engineering Toolbox

4. NASA Ingenuity Mars Helicopter Prepares for First Flight

5. Disclaimer: The simulation video an images were created from a geometry Ansys redrew from the public domain model of the helicopter and was run and post processed by an Ansys engineer. NASA JPL was not involved in their creation.

Developing CAE software systems for all simulation disciplines. Products: ANSA pre-processor/ EPILYSIS solver and META post-processor suite, and SPDRM, the simulation-process-data-and-resources manager, for a range of industries, incl. the automotive, railway vehicles, aerospace, motorsports, chemical processes engineering, energy, electronics…

BETA CAE Training

Basic and advanced training courses can be scheduled upon request. A variety of standard or tailored training schedules, per product or per discipline, are being offered to meet customers needs.

The training courses are given by highly experienced engineers of our Customers Service and the certified and authorized Services teams of our business agents.

Our training courses lead to a certification according to the course level and type.

A number of recommended training courses offered are described below. The list is not exhaustive and more courses can be designed according to your needs. Contact ansa@beta-cae.com for further details.

Upcoming Live Webinars

Beyond the numerous videos that we release every week, which allow you to enhance your knowledge upon demand, this is a new series of live webinar events that brings closer BETA and our friends. The events comprise talks, presentations and demos, on topics related to the use and deployment of our software for solving demanding problems in computational engineering. You are all welcomed to enjoy our webinars and take the most out of it by deepening your knowledge and broaden your horizons.

Upcoming Training Courses

Live on-line | BETA School for Simulation

2nd cycle - from April 5 to June 2, 2021
3rd cycle - from June 7 to August 6, 2021
4th cycle - from August 16 to October 20, 2021
5th cycle - from October 25 to December 29, 2021

Host: BETA CAE Systems India Pvt. Ltd.
Time Zone: IST

Duration: 2 months
Level: Basic & Intermediate
Fee: Upon request
Information: events@beta-cae.in

Job placement available upon the successful completion of the course.

GET THE BROCHURE

d3VIEW is a data to decision platform that provides out-of-the box data extraction, transformation and interactive visualizations. Using d3VIEW, you can visualize, mine and analyze the data quickly to enable faster and better decisions.

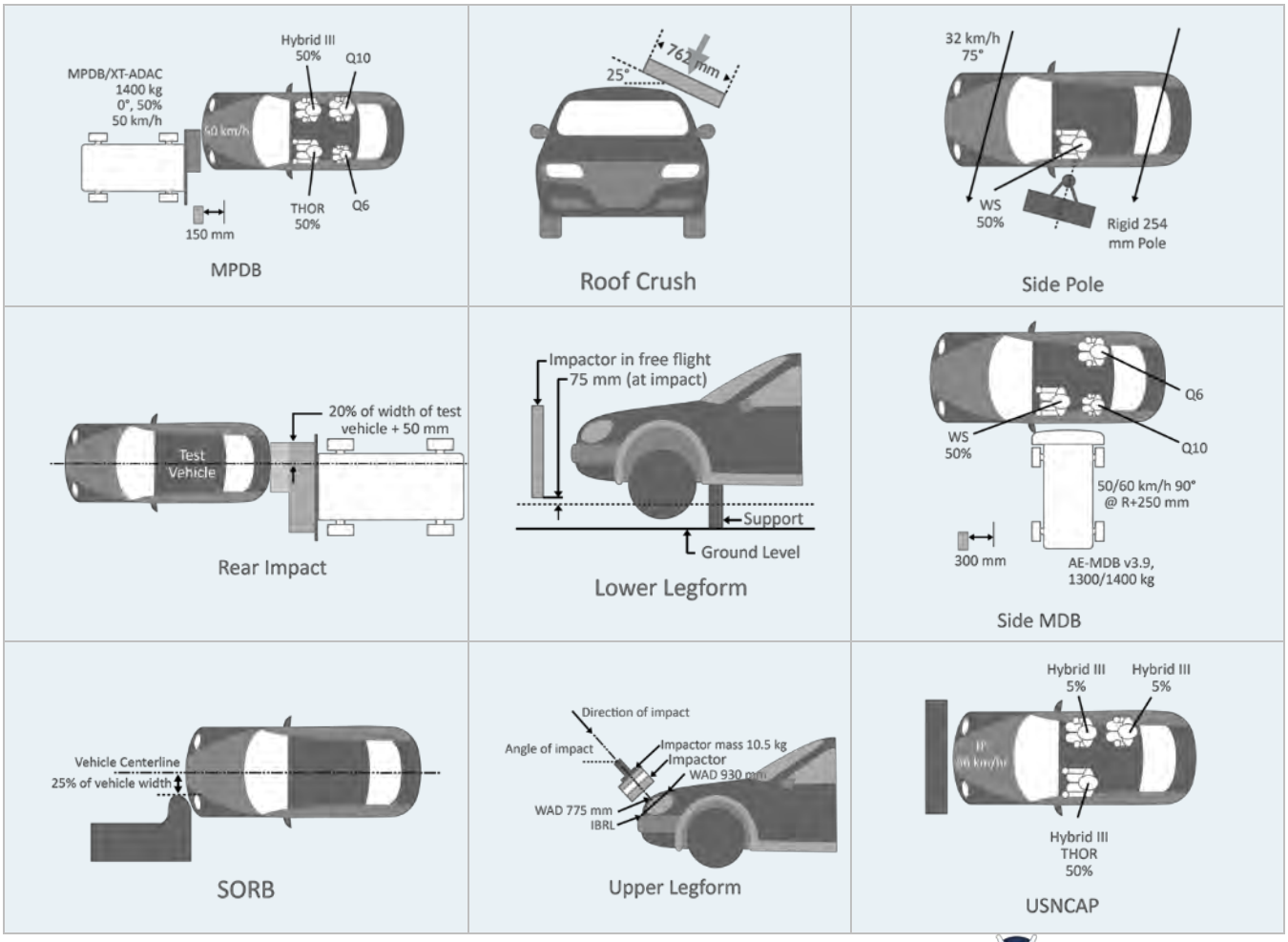

Accelerate Crashworthiness Engineering.

d3VIEW

www.d3view.com | support@d3view.com

Author: Christian Frech christian.frech@dynamore.de

Online and On-site Event! Submit your Abstract!

13th European LS-DYNA Conference
October 5-6, 2021, Ulm, Germany and online

Conference Website: www.dynamore.de/en/conf2021

Invitation
We kindly invite all users of LS-DYNA, LS-OPT, LS-PrePost and LS-TaSC as well as our dummy models to the 13th European LS-DYNA Conference at October 5-6, 2021 in Ulm, Germany, and online.

Online and On-site
Whether online or on site - the conference will be a great opportunity to talk with industry experts, catch up with colleagues and enjoy time exploring new ideas. In addition, attendees can meet with exhibitors to learn about the latest hardware and software trends as well as additional services relating to the finite element solver LS-DYNA, the optimization codes LS-OPT and LS-TaSC, and the pre- and postprocessor LS-PrePost.

Venue
Ulm is located directly on the A7 and A8 motorways and can be easily reached from Stuttgart and Munich airports.

Address:
Basteistraße 40
89073 Ulm
Telefon: +49 731 922990
Telefax: +49 731 9229930
www.ulm-messe.de

We will inform you about the online part as soon as possible.

Abstract submission
Please submit your abstract (maximum length 2,500 characters) by E-Mail to conf@dynamore.de or online at:
www.dynamore.de/en/2021-abstract

Important Dates
Abstract submission: May 28, 2021
Author notification: July 9, 2021
Paper submission: September 3, 2021
Conference date: October 5-6, 2021

Participant fees

Industry speaker:	420 Euro
Academic speaker:	360 Euro
Online speaker:	150 Euro
Industry:	640 Euro[1)] / 690 Euro
Academic:	490 Euro[1)] / 540 Euro
Online	200 Euro

[1)] Registration before 30 June 2021. All plus VAT.

Exhibiting and sponsoring
Please request further information.

Contact
DYNAmore GmbH
Industriestr. 2, D-70565 Stuttgart, Germany
Tel. +49 (0) 7 11 - 45 96 00 - 0
E-Mail: conference@dynamore.de
www.dynamore.de/en/conf2021

Author: Christian Frech christian.frech@dynamore.de

DYNAmore opens new branch office in Munich

New office in the capital of Bavaria

In March 2021 the DYNAmore GmbH has opened a new branch office in the Bavarian capital Munich. The team's activities at the new location focus on cooperation with automotive manufacturers, customers in the greater Munich area, and the Technical University. The new location is an important step for DYNAmore GmbH that helps to intensify and expand the cooperation with existing and new customers in the southern German area.

Strong need for the DYNAmore services

The company sees a lot of potential growth, as there is a strong need for the services in crash and metal forming simulation. As a result, DYNAmore expects to expand and hire new engineers in the near future.

(Office building of the new DYNAmore branch)

Method development and human modeling

In addition to general method development in LS-DYNA, the development of restraint systems and the topic of human modeling are the main focus of the engineers on-site. The cooperation with the Technical University of Munich, which is supported in several research projects, should also be mentioned.

Investing in research is part of the corporate philosophy at DYNAmore. There are excellent specialists in the field of numerical simulation and constitutive modeling at the TU Munich. DYNAmore is very much looking forward to the collaboration and many exciting projects.

The new office is located at the following address:

DYNAmore GmbH
Oskar-Schlemmer-Straße 11
80807 München, Germany

DYNAmore GmbH is very happy about the opening of the new office and is looking forward to the new tasks and challenges of the future.

DYNAmore Headquarters

DYNAmore GmbH
Industriestrasse 2
D-70565 Stuttgart
www.dynamore.de
info@dynamore.de

Author: Christian Frech christian.frech@dynamore.de

Webinars and on-demand Video-Seminars 2021

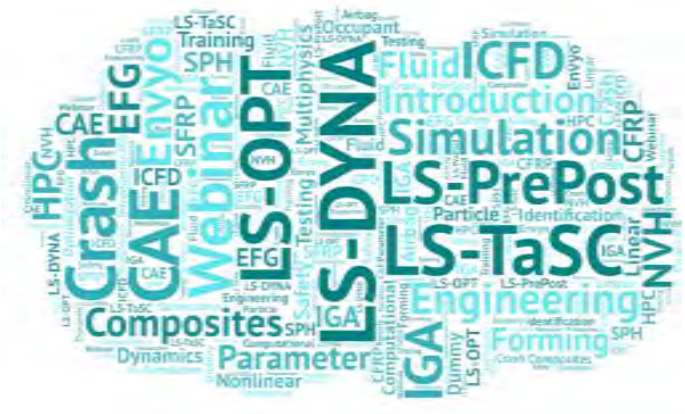

Online trainings in May and June

Webinars	
Introduction to LS-DYNA	4-6 May, 26-28 May 30 June-2 July
Introduction to PRIMER for LS-DYNA	4-5 May
Introduction to LS-DYNA	4-6 May
NVH	10-11 May
CESE Compressible Fluid Solver	17-18 May
ALE and FSI	19-21 May
CPM Airbag Modelling	11 June
La rupture dans LS-DYNA : d'une utilisation simple aux modélisations avancées	17 June
Discrete Element Method	23-24 June
Video Seminars	
Introduction to LS-DYNA online	anytime
Introduction to LS-DYNA Compact	anytime
Introduction to LS-PrePost	anytime
Crashworthiness Simulation with LS-DYNA	anytime
Modeling Metallic Materials	anytime
LS-OPT - Optimization	anytime
LS-OPT - Robustness	anytime

Visit our website for complete overview and registration www.dynamore.de/en/seminars

A leading innovator in Virtual Prototyping software and services. Specialist in material physics, ESI has developed a unique proficiency in helping industrial manufacturers replace physical prototypes by virtual prototypes, allowing them to virtually manufacture, assemble, test and pre-certify their future products.

Empower Automakers to Engineer and Manufacture Multi-Material Assemblies with Confidence

Virtual Prototyping represents an end-to-end approach for early validation of material and design choices, manufacturing and assembly process strategy, with significant benefits over the complete body development cycle.

Wednesday, April 7, 2021
By Matthieu Niess

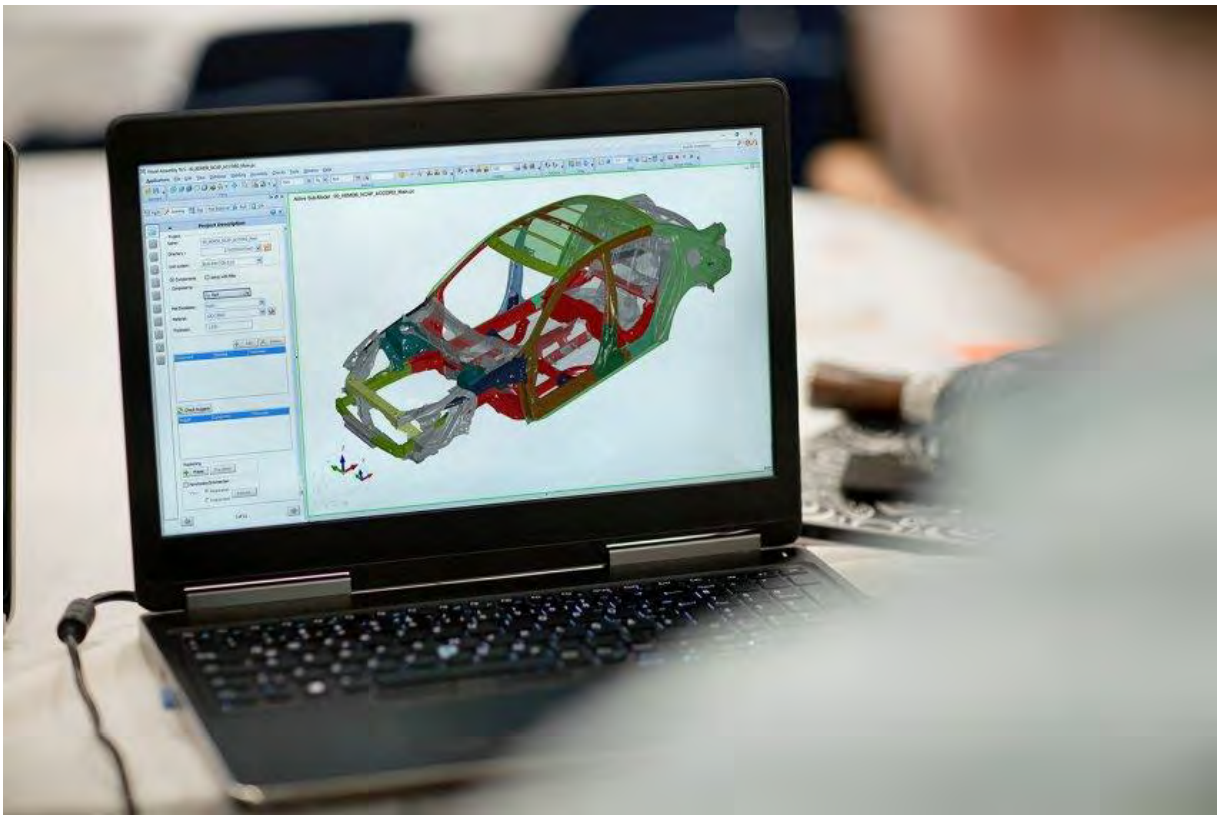

Automotive companies strive to develop disruptive and sustainable mobility devices. Their carbon reduction objectives mostly translate into weight reduction targets – which conveniently fits the bill for increasing EV range. Introducing new materials and processes can be very tricky with regards to feasibility, as much as for final product performance that no one is ready to jeopardize. Not to mention cost – product development involving new materials and processes over which you have no experience is inevitably risky and full of surprises. Read on to learn about feasibility assessments, assembly process prediction, performance validation – all-virtual, cost-effective and “first time right”.

Shifting from single-point numerical simulation to end-to-end Virtual Prototyping

Over the past decades, numerical simulation has been instrumental in allowing OEMs to evaluate manufacturing feasibility and to assess and validate a design's performance. However, body manufacturing decisions are made relatively late in the process, after the design freeze, and automakers still rely heavily on physical testing. Often, engineers detect body assembly distortions too late in the process (image 1).

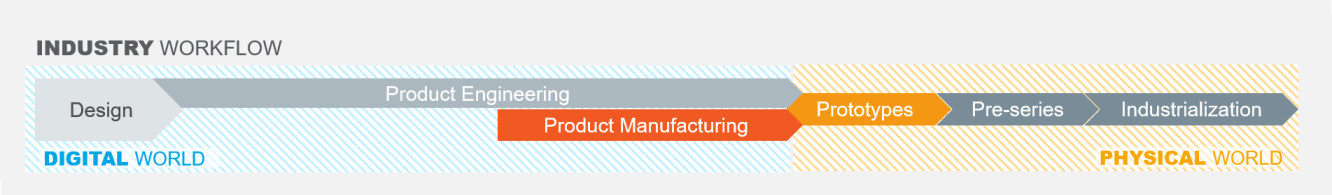

The ambition to frontload manufacturing decisions is not new. But the design-to-cost requirement brings an additional push. Indeed, the best practice is to find an optimal design as early as possible and to validate it in the engineering phases, and this in a highly predictive manner, to avoid costly prototypes and late design changes during manufacturing pre-production validation.

Achieving such an optimal design through a purely digital approach is not straightforward. Two main aspects need to be accounted for to ensure a fluid journey until serial production (image 2).

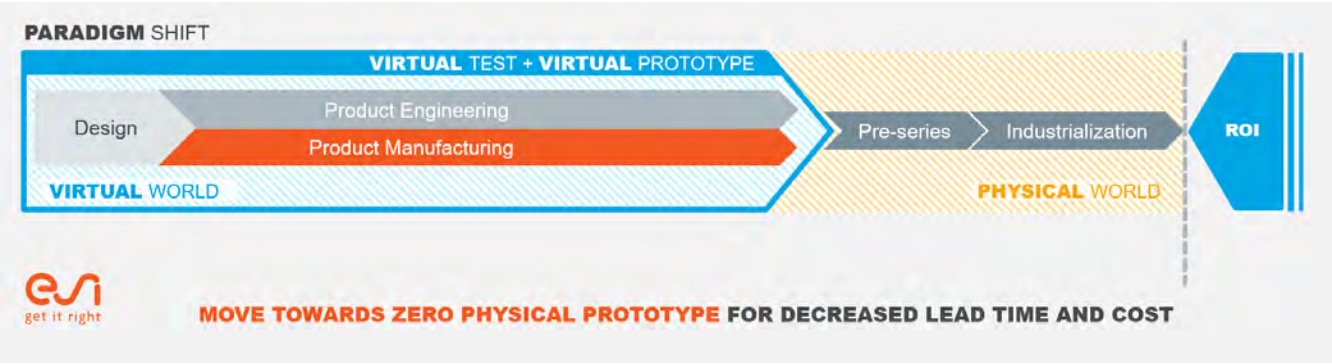

Single Parts Manufacturing: Detailed simulation of single-part manufacturing has been established in the industry for many years. However, typically it comes later in the workflow because engineers need to define various tool environments first. With the rise of advanced mix-materials, automakers, need early confidence to make the right decisions about which material works best at which place. Thus, it is very important to be able to estimate the manufacturing feasibility since the beginning, when the first CAD data and bill of material (BOM) are generated. Virtual Prototyping allows engineers to consider all this information in early development phases and therewith improving the predictivity of the function and performance validation as well as the assembly process simulation – even prior to process tools and dies definitions.

Joining Process: The possibilities to join multi-material assemblies are numerous. To find the right match, it is crucial to accurately model and simulate the joining process in order to transfer the connection strength into crash and durability optimization. In addition, engineers need to account for the impact of the joining process on the parts' geometries in order to predict assemblies' quality. The final target is always to have the best predictivity as early as possible, with minimum computation time.

In the later pre-production validation phase, the first physical parts would be sent over typically from different suppliers and locations to OEM assembly plants in order to check final assembly tolerances and quality. To overcome these costly logistics, Virtual Prototyping allows engineers to use instead 3D scans of the single parts plus the joining process impact as input for their assembly simulation. Consequently, parts and assemblies tolerances deviations can be anticipated and costly trial-and-error phases avoided.

Furthermore, 3D scans can even be replaced now by digital results of manufacturing processes, like stamping. As a consequence, distortions and tolerances in body and chassis, as well as perceived quality in class A panels assemblies, can be analyzed and predicted already in early development phases, ensuring the end product can be produced and assembled at the highest quality standard within the specified tolerance range.

In a nutshell: Virtual Prototyping represents an end-to-end approach, for early validation of material and design choices, manufacturing and assembly process strategy, with significant benefits over the complete body development cycle. It empowers automakers to effectively validate all the leading lightweight material candidates for vehicle structures safety-critical components and to associate the optimum joining processes to achieve assemblies at the best performance/cost/quality ratio.

This robust foundation brings early confidence before moving to the physical world with clarity about the right production strategy, which is finally virtually validated prior to production with a constant link to function and performance validation. This paves the way for a digital Body factory in which automakers can progress towards zero physical prototypes, ultimately shortening the overall product development cycle and minimizing its cost and time to start of production (SOP).

Discover our software solution here.

Join **our upcoming Multi-Material Joining Assembly Webinar Series** to find out how to couple the engineering and the manufacturing world in order to make the right choice as early as possible.

Customer Success: Nissan reduced engineering lead times for new lightweight material by as much as 50%

To address the weight reduction objectives of Nissan's Green Program, the Japanese OEM has been investigating mixed material use (aluminum, steel, and composites assemblies). Nissan engineers used ESI simulation solution for composites manufacturing to develop a new process method of injection molding and compressed molding, bringing significant efficiency gains for their production lines. By trading the usually long and costly trial-and-error period for developing a new manufacturing process with numerical simulation, Nissan's engineers managed to make early decisions on lightweight material types, while securing design requirements and production goals. By their estimation, they succeeded in reducing engineering lead time by as much as 50%.

In terms of manufacturing results: just before ESI kicked off its first-ever ESI Live conference back in November 2020, Nissan publicly announced their breakthrough in carbon fiber parts production. They went from producing a Carbon-Fiber Reinforced part in two hours down to 2 minutes, reducing production time for a single molding by 80%. This technological agility also allows Nissan to produce complex part shapes enabling an average weight reduction of 80kg per vehicle.

Such an achievement became possible not at least thanks to the ability of confident decision-making and early optimization and thanks to synchronized activities in both design and manufacturing engineering for forming, heat treatment, joining and assembly processes.

Read the full story here

ETA has impacted the design and development of numerous products - autos, trains, aircraft, household appliances, and consumer electronics. By enabling engineers to simulate the behavior of these products during manufacture or during their use, ETA has been involved in making these products safer, more durable, lighter weight, and less expensive to develop.

DYNAFORM

DYNAFORM 6.0 is the sixth-generation DYNAFORM product. It provides a user-friendly and intuitive interface with a streamlined design. The analysis process is fully based on the stamping process, which requires less CAE knowledge, and minimum geometry and element operations. This latest release offers the following features and improvements:

- Intuitive and Streamlined Interface
- Tree Structure to Manage Operation
- Simulation Data Manager
- Customized Icons Grouping for Drop-down Menu Functions
- Separate and Independent Application
- Unified Pre and Post Processing
- Multi-Window View
- Access Functions Using Right Mouse Button Clicks
- Supports Large Forming Simulation Models
- Geometry Manager
- Process Wizard for Blank Size Engineering
- Minimum Geometry and Elements Operations
- New Material Library Window
- New Drawbead Shape and Library
- Coordinate System Manager
- Instant Section Cut
- Tata Steel FLD
- Balloon Label
- PowerPoint and Excel Based Automatic Formability Report Generation

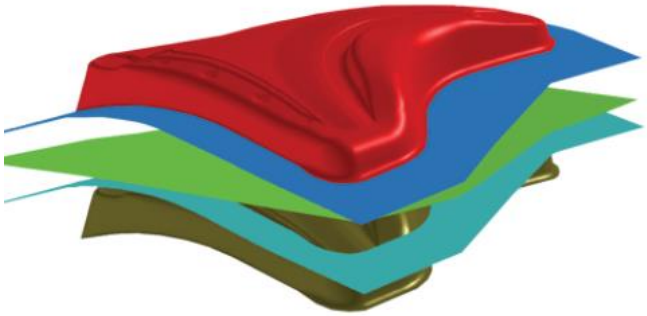

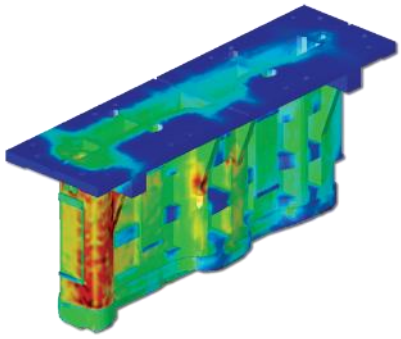

Highlights from our FEA Not To Miss Software & Engineering Solutions ISSN 2694-4707 and FEA Not To Miss Website - Sign up for our Monthly Magazine via email

FEA Not To Miss choice for April - Each Ansys course includes videos, handouts, practice or homework problem sets and short quizzes. So, let's head on over and remember to bring your favorite coffee, tea or soda (sugar free).

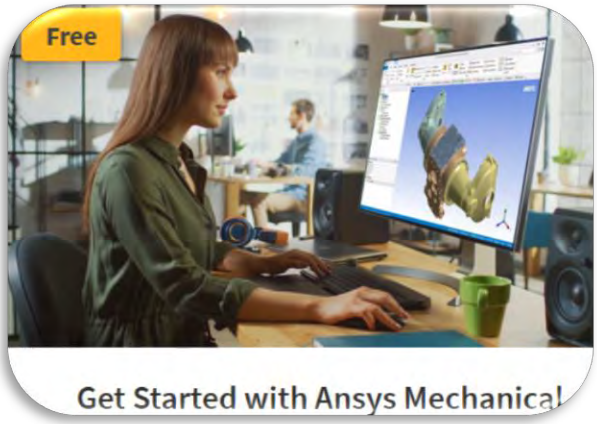

Get Started with Ansys Mechanical - When working with any computer-aided engineering software, it is important to understand its workflow and user interface so you can be more productive and efficient when performing your analysis in the software. In this course, you will get familiar with the Ansys Mechanical user interface and learn important tips and tricks to be more productive with your simulation workflow.

Fundamental Topics in Contact - Unlike the real world, bodies do not automatically interact with each other in numerical simulations. In order to model those interactions, proper contact definition between the bodies is required. This course discusses a few fundamental topics in contact and demonstrates the use of Ansys Mechanical software in modeling contact.

Webinar Not To Miss

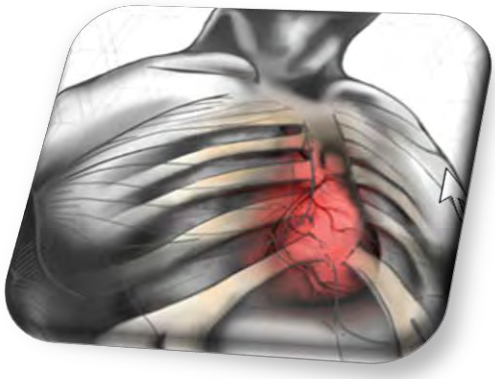

May 18th

In Silico Design and Approval for Cardiovascular Devices | Ansys Webinar

Computer-aided simulations are proving to be particularly promising in accelerating the regulatory process and simultaneously can have the benefit of increasing patient safety by investigating scenarios not possible with traditional methods.

Shanghai Hengstar & Enhu Technology sells and supports LST's suite of products and other software solutions. These provide the Chinese automotive industry a simulation environment designed and ready multidisciplinary engineering needs, and provide a CAD/CAE/CAM service platform to enhance and optimize the product design and therefore the product quality and manufacture.

Online workshop for basic of LS-DYNA

Shanghai Hengstar Technology will organized a Web Training of the basic in LS-DYNA on Mar 24 2021.

Contents:

1. Introduction of LS-DYNA
2. Control card
3. Instructions of LS-PrePost
4. Output files and data
5. Element Type
6. Time `step` and CPU time
7. Selection of material model
8. Hourglass
9. Loading and setting initial conditions
10. Connect
11. Boundary condition
12. Damping application
13. Contact settings
14. Finite element model evaluation
15. Exercise

Instructor:

Jun Liu (Senior Engineer)
Jun Liu was graduated from Tongji University in 2008 in vehicle engineering. He has been engaged in automobile R & D industry for more than ten years, and has rich experience in automobile safety performance research and simulation. He has accumulated a lot of pre-processing and post-processing techniques for FRB, ODB, aemdb collision modeling and simulation analysis. And He has a lot of experience in simulation and optimization of five-star vehicle development process . Also can master LS- DYNA and ansa, meta, HyperMesh, hyperview, primer and other pre-processing software.

Duration and Style:(7 hours web training): Mar 24 (9:00AM-17:00PM) **Language:** Mandarin

Contact: Xixi Fei Tell:021-61630122 mobile:13524954631 Email:Training@hengstar.com

Shanghai Hengstar Technology Co., Ltd
hongsheng@hengstar.com
http://www.hengstar.com
Shanghai Enhu Technology Co., Ltd
http://www.enhu.com

JSOL supports industries with the simulation technology of state-of-the-art. Supporting customers with providing a variety of solutions from software development to technical support, consulting, in CAE (Computer Aided Engineering) field. Sales, Support, Training.

LS-DYNA Features

LS-DYNA opens the nonlinear world

The phenomena adopted for developing product designs are becoming increasingly complex: automotive crashes, metal forming, forging, large deformations of rubber materials, and failure of plastic parts. CAE simulation is now an essential tool for attaining a complex and high-quality design in various industries. LS-DYNA was originally introduced by Dr. John O. Hallquist at the Lawrence Livermore National Laboratory in the 1970s. In the late 1980s, Livermore Software Technology, LLC (LST, LLC) was founded to develop LS-DYNA as a commercial code. LST, LLC has been committed to developing LS-DYNA for solving nonlinear problems more precisely and stably. LS-DYNA is now known worldwide as one of the best nonlinear solvers and is used in both the academic and the industrial worlds.

KAIZENAT Technologies Pvt Ltd is the leading solution provider for complex engineering applications and is founded on Feb 2012 by Dr. Ramesh Venkatesan, who carries 19 years of LS-DYNA expertise. KAIZENAT sells, supports, trains LS-DYNA customers in India. We currently have office in Bangalore, Chennai, Pune and Coimbatore.

Internal Cooling of Turbine Blade – CFD Analysis

Objective: To perform Pin Fin cooling for internal turbine blades placing rib turbulators. Results of flow turbulence is observed which covers more surface area for better temperature distribution and internal cooling process of Turbine blade.

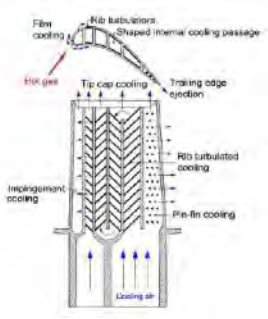

Gas Turbine with Cooling system

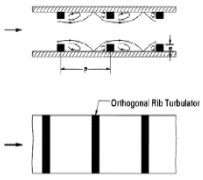

Ribs induced into flow domain

Modelling:

Design and meshing of Internal channel of Turbine blade fluid domain have been performed in ANSYS Tool.

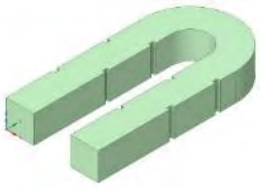

Methodology:

Structured mesh with optimum quality.

ANSYS Fluent workflow:

- Pressure based scheme
- Steady state analysis
- K-Omega Turbulence model
- Energy equation –ON
- Material: Air
- Boundary conditions:
- Inlet

Velocity: 1 m/s

Temperature: 285 K

- Wall

Temperature: 370 K

- Operating Pressure: 101325 Pa

Results:

Velocity Profile:

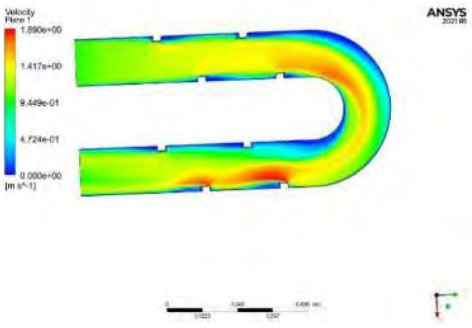

Temperature profile:

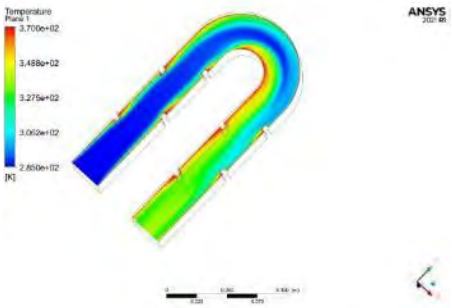

An effective level of convective heat transfer is observed inside fluid domain.

Ending Remarks:

1. We can notice the rate of heat transfer exchange in the fluid domain.
2. This occurs only due the turbulence of flow created due to ribs placed inside as noticed in velocity profile.
3. As the flow gets obstructed due to ribs which leads to the flow contacting more cross section area of the domain through which heat exchange happens.

Contact

Email : support@kaizenat.com
Phone: +91 80 41500008

A team of engineers, mathematicians, & computer scientists develop LS-DYNA, LS-PrePost, LS-OPT, LS-TaSC, and Dummy & Barrier models, Tire models.

On Setting up a 2D Structured ALE Model

Hao Chen, Ansys

LS-DYNA ALE has been widely used to simulating moving fluids interacting with structures. Unlike CFD, the focus is rather on the structure response under dynamic loading from fluids, than the fluids' motion. Fluids are agitated by a high pressure gradient; and then hit the structure, carrying a large momentum. The key in successfully capturing the physics lies in the fluid-structure interaction algorithm. It needs to accurately predict the peak of pressure loading during the impact, which is characterized as a momentum transfer process. This request could only be fulfilled by a transient analysis with a penalty-based coupling between fluids and structure.

In 2015, LSTC introduced a new structured ALE (S-ALE) solver option dedicated to solve the subset of ALE problems where a structured mesh is appropriate. As expected, recognizing the logical regularity of the mesh brought a reduced simulation time for the case of identical structured and unstructured mesh definitions. It also comes with a cleaner, conceptually simpler way of model setup.

Since the past year, efforts have been made to expand S-ALE into the 2D territory. This would be beneficial to both users and the developer. Using a single set of coding for both 3D and 2D models would greatly simplify the maintenance. In the meantime, it also provides a unified platform for future developments. As S-ALE 3D coding has been tested intensively during the last five years, we believe the S-ALE 2D solver would be stable and efficient from the beginning. For users, using the same set of keywords in both 3D and 2D applications could reduce the learning time and modeling efforts so they could focus more on the physical part of the modeling.

This article gives a brief description of the S-ALE 2D model setup.

Three step setup

We follow a straight-forward three step setup. First, mesh; secondly, material properties of fluids; thirdly, filling the mesh with fluids. In this section, we describe the three keywords doing these three steps.

1. Mesh generation: *ALE_STRUCTURED_MESH; *ALE_STRUCTURED_MESH_CONTROL_POINTS

In S-ALE, mesh is always rectangular. To determine the mesh layout in the space, we need the following information:

a. Mesh spacing along three axes (LCIDX,LCIDY,LCIDZ) in 3D; two axes (LCIDX,LCIDY) in 2D.
b. The origin (NID0), and local coordinate system (LCSID).

Other fields are for identification purpose only and are self-explanatory. MSHID stands for mesh ID; DPID Part ID; NBID and EBID are the IDs of first S-ALE mesh node and element, respectively. TDEATH is to the "death time" for S-ALE mesh. It is to turn off the S-ALE calculation once the most of fluid loading is applied; and keep the Lagrange model running as the structure deformation is not fully developed yet.

*ALE_STRUCTURED_MESH							
MSHID	DPID	NBID	EBID				TDEATH
CPIDX	CPIDY	CPIDZ	NID0	LCSID			

The CPIDX, CPIDY and CPIDZ are IDs of *ALE_STRUCTURED_MESH_CONTROL_POINTS cards. Each card specifies the mesh spacing along one axis.

*ALE_STRUCTURED_MESH_CONTROL_POINTS							
CPID							
N1		X1		RATIO1			
…		…		…			
Nn		Xn		RATIOn			

In a 2D simulation, the mesh is 2 dimensional so CPIDZ is no longer needed. Nonzero value of CPIDZ would be simply ignored and hence harmless. For 2D Axisymmetric case, special caution needs to be taken when using NID0 (origin shift) and LCSID (mesh rotation) feature, to make sure the created mesh is not in conflict with the assumption that the axis of symmetry is at x=0.

2. Material definitions: *ALE_STRUCTURED_MULTI-MATERIAL_GROUP_?

S-ALE mesh is simply a spatial domain in which fluids flow. In order to let the code know what and how many fluids there are, we need to provide material properties of each fluid and list them all under the card *ALE_STRUCTURED_MULTI-MATERIAL_GROUP. Please note, AMMG stands for ALE multi-material group, a rather alternative and maybe confusing name for "ALE fluid". In this paper we are going to use AMMG and fluid interchangeably.

For 2D, *ALE_STRUCTURED_MULTI-MATERIAL_GROUP also carries another role. It is to specify the nature of the 2D simulation (element formulation), i.e. Plane strain or Axisymmetric. An

option string at the end, either PLNEPS or AXISYM does the job. These two options directly correspond to setting elform=13 and elfrom=14 in *SECTION_ALE2D card.

*ALE_STRUCTURED_MULTI-MATERIAL_GROUP_PLNEPS/AXISYM							
AMMGNM1	MID1	EOSID1					PREF1
…	...	…					…
AMMGNMn	MIDn	EOSIDn					PREFn

"AMMGNM" is a name one gives to a AMMG (ALE Multi-Material Group), aka ALE fluid. It is used in other cards, for example, *SET_MULTI-MATERIAL_GROUP_LIST to refer to that AMMG. "MID" and "EOSID" are the material ID and EOS ID, respectively.

"PREF" is to describe the reference pressure or "base pressure" of that fluid. This might be somewhat new to our typical users from solids background. Pressure of a solid material, if not preloaded, always starts from zero. In such case, its reference pressure or base pressure, is zero. But most fluids have non-zero reference pressure. For example, air has a base pressure of 101325 Pa (1 bar atmospheric pressure). Traditionally this reference pressure is prescribed using the field "PREF" in *CONTROL_ALE card. The new *ALE_STRUCTURED_MULTI-MATERIAL_GROUP has a design to allow each AMMG to have its own reference pressure. The author believes this added flexibility could be proven very useful in certain applications.

3. Volume Filling: *ALE_STRUCTURED_MESH_VOLUME_FILLING

We created a rectangular 2D S-ALE mesh in step 1 and came up multiple fluids (AMMGs) definitions in step 2. We now fill the mesh with those fluids. We do that by specifying which fluid occupies either inside or outside of certain geometry. These geometries could be simple shapes like sphere, plane, box, cylinder. Or it could be user-defined complex shape like structure surfaces.

This is done by using the keyword "*ALE_STRUCTURED_MESH_VOLUME_FILLING". The "volume filling" process typically is done through multiple "tasks", each task by a separate keyword.

*ALE_STRUCTURED_ MESH_VOLUME_FILLING							
MSHID		AMMGTO		NSAMPLE			VID
GEOM	IN/OUT	E1	E2	E3	E4		

MSHID is the S-ALE mesh ID, defined in *ALE_STRUCTURED_MESH card. And AMMGTO is the name of ALE fluid to be filled, defined in *ALE_STRCUTURED_MULTI-MATERIAL_GROUP. VID is to prescribe the initial velocity of that fluid, if any. And NSAMPLE is default to 3 which means

that one ALE cell is divided into 7x7x7 (7=2*3+1) sub-cells in 3D and 7x7 in 2D and each sub-cell is checked to see if it is inside/outside.

It supports 5 basic geometries: Plane, Cylinder, Ellipsoid, Box with indices and Box with coordinates. And E1-E4 are used to provide information of these geometries. For complicated geometries, we need users to provide us with a segment set (or something we could internally convert to a segment set). The assumption is that all segment normals are consistent; and those normals point to the "inside". For convenience, we provide a "IN/OUT" flag for an easier flip.

Boundary/Initial Conditions and *CONTROL_ALE

Boundary Conditions. The most used type of boundary condition is single point constraint (SPC). It is to constrain motion at a point (node) along certain direction. Traditionally, we use *BOUNDARY_SPC to apply SPC constraints in S-ALE. In R12.1 (Ansys 2021R2), we added a new "macro-like" keyword "*BOUNDARY_SALE_MESH_FACE" to make this process more user-friendly.

*BOUNDARY_SALE_MESH_FACE							
OPTION	MSHID	-X	+X	-Y	+Y	-Z	+Z
SYM	1			1			
NOFLOW	1					1	1
NONREFL	1	1	1		1		

Three options, SYM, NOFLOW and FIXED, are for SPC constraint. SYM and NOFLOW, are doing the same thing. That is to constrain the flow perpendicular to the plane. We have both options available, simply to provide a one-to-one match between the options and real physical scenarios. FIXED is to fix all nodal motions at that face.

The other one, NONREFL, is to apply non-reflecting boundary at S-ALE mesh face(s). Internally this option is translated to *BOUNDARY_NON_REFLECTING + *SET_SEGMENT.

Initial conditions. IC setup is relatively simple. Typically it is only to assign some initial velocity to some nodes. Most commonly, initial velocities are applied simultaneously with volume filling process, through the *ALE_STRUCTURED_MESH_VOLUME_FILLING card. Like the following:

```
*ALE_STRUCTURED_MESH_VOLUME_FILLING
$#   mshid         -    ammgto         -   nsample         -         -       vid
         1               plate                                              1
$#    geom    in/out     boxid
BOXCOR             0         1
```

And the initial velocity (vx=-61.631,vy=208.06) is prescribed by using the *DEFINE_VECTOR card.

```
*DEFINE_VECTOR
$#     vid        xt        yt        zt        xh        yh        zh       cid
         1   -61.631    208.06       0.0       0.0       0.0       0.0         0
```

Control Card. *CONTROL_ALE is used to set up certain global control parameters in a S-ALE simulation. The only relevant parameters are: NADV and METH. METH=1/2 controls the order of advection scheme, 1st or 2nd order. NADV could be adjusted to increase the interval (in number of cycles) between two advections. It is to provide users with a way to shorten the running time for problems in which deformation is small compared to element size in one cycle. Then we could wait until the element is severely deformed and then perform an advection (remapping). All other parameters most cases the user could safely ignore.

```
*CONTROL_ALE
$#     dct       nadv       meth       afac       bfac       cfac       dfac       efac
                    1          1 -1.000000
$#   start        end      aafac      vfact       prit        ebc       pref     idebc
```

The parameter PREF was to set the reference pressure. However, S-ALE came up with a better design to allow users to prescribe reference pressure for each ALE fluid (AMMG) through "PREFn" in *ALE_STRUCTURED_MULTI-MATERIAL_GROUP. PREF will still be kept there for backward compatibility but we strongly recommend setting reference pressure through the *ASMMG card.

Example

Now let us use a simple example to illustrate the 2D S-ALE setup. We have a rigid body wedge composed of beam elements slamming into water as the figure shown below. It is a 2D plane strain model. The unit used is mm-ton-s. Pressure unit is Mpa.

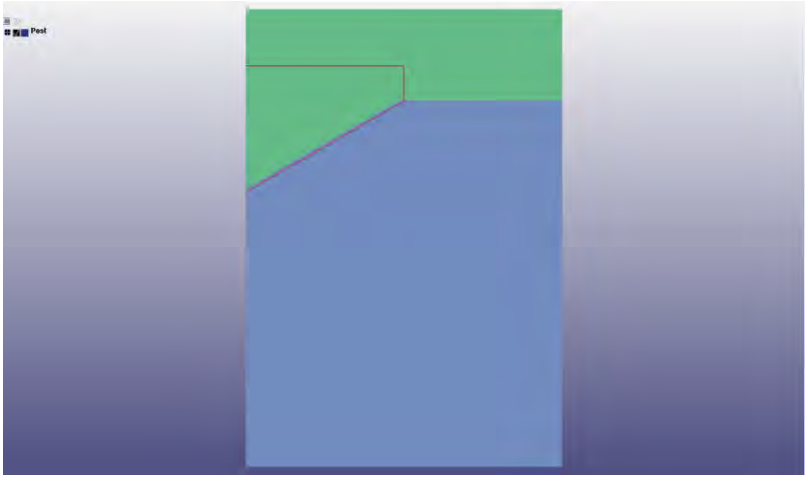

Step 1: To construct a mesh spans (0,-433.013) to (500,288.675) with 100x150 elements.

```
*ALE_STRUCTURED_MESH
$    mshid       pid      nbid      ebid
         1        11    100001    100001
$    cpidx     cpidy     cpidz      nid0     lcsid
      1001      1002      1003
*ALE_STRUCTURED_MESH_CONTROL_POINTS
      1001
$                x1                  x2                  x3                  x4
                  1                 0.0
                101               500.0
*ALE_STRUCTURED_MESH_CONTROL_POINTS
      1002
$                x1                  x2                  x3                  x4
                  1            -433.013
                151             288.675
*ALE_STRUCTURED_MESH_CONTROL_POINTS
      1003
$                x1                  x2                  x3                  x4
                  1                -0.5
                  2                 0.5
```

Here CPIDZ is harmless. All nodal coordinates will be initialized with z=0. We will see its purpose later.

Step 2: Set up ALE multi-material Groups (AMMGs or ALE fluids). There are totally 2 AMMGs defined. First is "water" by *MAT_NULL (MID=4) and *EOS_LINEAR_POLYNOMIAL (EOSID=4). The second is "air" by * MAT_NULL (MID=5) and *EOS_LINEAR_POLYNOMIAL (EOSID=5). Their materials properties are given as follows.

```
*MAT_NULL
$#     mid        ro        pc        mu     terod     cerod        ym        pr
         4  1.026e-9       0.0       0.0       0.0       0.0       0.0       0.0
*EOS_LINEAR_POLYNOMIAL
$#   eosid        c0        c1        c2        c3        c4        c5        c6
         4       0.0       2.3       0.0       0.0       0.0       0.0       0.0
$#      e0        v0
       0.0       0.0
*MAT_NULL
$#     mid        ro        pc        mu     terod     cerod        ym        pr
         5 1.293e-12       0.0       0.0       0.0       0.0       0.0       0.0
*EOS_LINEAR_POLYNOMIAL
$#   eosid        c0        c1        c2        c3        c4        c5        c6
         5       0.0       0.0       0.0       0.0       0.4       0.4       0.0
$#      e0        v0
       0.0       0.0
```

Here for simplicity, we assigned initial pressure to be zero for both air and water. In problems where the air compressibility becomes important, we could prescribe the initial pressure of 1 bar by assigning e0=0.101325/0.4=0.258125. If we do that, please do not forget to set the reference pressure of water to 1 bar by making PREF=0.101325 in *ALE_STRUCTURED_MULTI-MATERIAL_GROUP (*ASMMG) otherwise water pressure is not well balanced.

Now construct the ALE fluids by using *ALE_STRUCTURED_MULTI-MATERIAL_GROUP. And specify the nature of the simulation to 2D plane strain by adding option _PLNEPS at the end.

```
*ALE_STRUCTURED_MULTI-MATERIAL_GROUP_PLNEPS
$     name       mid     eosid                                          pref
   water           4         4
  air              5         5
```

Step 3: Volume Filling the initial S-ALE mesh. By *ALE_STRUCTRUED_MESH_VOLUME_FILLING.

First, fill all with “water”.

```
*ALE_STRUCTURED_MESH_VOLUME_FILLING
$#   mshid          -    ammgto         -   nsample         -         -     vid
         1             water
$#    geom    in/out
ALL
```

Next, switch above the plane to “air”.

```
*ALE_STRUCTURED_MESH_VOLUME_FILLING
$#   mshid          -    ammgto         -   nsample         -         -       vid
         1              air
$#    geom    in/out      nid1      nid2
 PLANE                   10001     10002
*NODE
$#   nid               x               y               z       tc      rc
   10001             0.0         144.338
   10002             0.0         145.338
```

Finally, we switch the fluid inside the wedge to “air”.

```
*ALE_STRUCTURED_MESH_VOLUME_FILLING
$#   mshid          -    ammgto         -   nsample         -         -     vid
         1              air
$#    geom    in/out    ssetid
 SEGSET            1         1
```

Boundary Conditions and *CONTROL_ALE card

```
*BOUNDARY_SALE_MESH_FACE
$   option     mshid        -x        +x        -y        +y        -z        +z
    NOFLOW         1         1         1         1         1         1         1
```

Here we also set the SPC constraints at -z and +z mesh faces. It is not necessary but generally harmless. We will see why we did that in a minute.

```
*CONTROL_ALE
$#     dct      nadv      meth      afac      bfac      cfac      dfac      efac
                            1
$#   start       end     aafac     vfact      prit       ebc      pref   nsidebc
```

Remember how we want our users to be minimalist on *CONTROL_ALE?

FSI Setup

In the next R12.1 (Ansys 2021R2) release, *ALE_STRUCTURED_FSI card becomes fully functional with added 2D support. And here we are using this much simpler, stabler card embedded with a better leakage control algorithm.

```
*ALE_STRUCTURED_FSI
$#    slave    master     sstyp     mstyp                                    mcoup
         1        11         2         1                 4                  -123
$#    start       end      pfac                       flip
        0.0       0.0        -1
*SET_MULTI_MATERIAL_GROUP_LIST
$#  ammsid
        123
$# ammgid1   ammgid2   ammgid3   ammgid4   ammgid5   ammgid6   ammgid7   ammgid8
   water
*DEFINE_CURVE
$#     lcid
         1
$#                a1                  o1
                 0.0                 0.0
                 1.0                 1.0
```

Simply put, what we did in the above cards is as follows:

1. Couple a segment set (sstyp=2) with id 1 (slave=1) to "water" (mcoup=-123) in the S-ALE mesh part (mstyp=1) with id 11 (master=11).
2. Specify the couple stiffness to use the load curve id 1 (PFAC=-1). This load curve establishes a linear relationship between penetration and penalty spring pressure. It comes with two points. The first is always (0,0) which means no penalty pressure is given when the penetration is zero. The second point we recommend (0.1xdl, p_max). This is to tell the FSI algorithm to apply the p_max on coupling surface when fluids penetration is around 1/10 of the S-ALE element size. P_max is the maximum impact pressure that users need to come up with their own guess/estimate. The load curve used here instructs FSI to apply a penalty pressure of 10 bars at a penetration of 1 mm. We did not follow the rule here only because the toy nature of this simple model.

Below is the water and wedge at t=0., t=7.5ms and t=15ms. The input deck is available at https://ftp.lstc.com/anonymous/outgoing/hao/sale/models_R121/slam_wedge/. It took only 2 seconds to run this model with my 16 core machine.

Axisymmetric and 3D models

Here we show how easy we could switch between Plane Strain, Axisymmetric and 3D simulations. First let us change this plane strain model to an axisymmetric one. All we need to do is to replace PLNEPS by AXISYM in the *ASMMG card.

```
*ALE_STRUCTURED_MULTI-MATERIAL_GROUP_AXISYM
$     name       mid     eosid                                          pref
   water           4         4
  air              5         5
```

For Lagrange part of the model, we need to change the beam element formulation from 7 (plane strain) to 8 (axisymmetric). And that is it!

```
*SECTION_BEAM
$#   secid    elform
         1         8
$#      t1        t2        t3        t4
       1.0       1.0       1.0       1.0
```

Now we change it to a 3D model. All we need to do is to strike out _PLNEPS from the *ASMMG card.

```
*ALE_STRUCTURED_MULTI-MATERIAL_GROUP
$     name       mid     eosid                                          pref
   water           4         4
  air              5         5
```

Of course, for LAG part, we need to prepare a different set of mesh with different nodes and elements defined. The model input deck contains both 2D and 3D Lagrange mesh and one could include the corresponding mesh files.

```
*INCLUDE
$mesh_wedge_2d.k
mesh_wedge_3d.k
```

3D simulation is a little bit more costly – 5 seconds on my 16 core machine. So we urge the reader to download the test case input deck and play with the switching between plane strain, axisymmetric and 3D simulations. We promise it is going to be fast and easy!

Below figure compares FSI pressure between plane strain and 3D simulations. We could see these two curves almost on top of each other. This validates the newly developed 2D S-ALE works as expected.

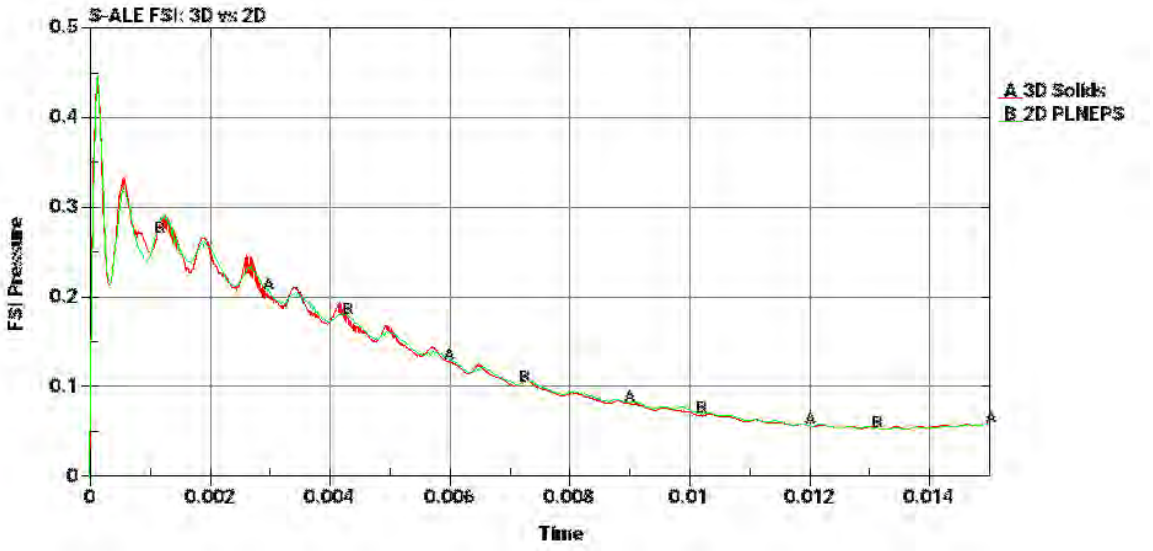

Ending Remarks

LS-DYNA ALE module has been known for its steep learning curve. Partially it was because setting up Eulerian models are intrinsically different from Lagrange models. But the design of ALE keyword cards, for sure, has caused quite a lot of confusions among our users, new and experienced.

To prompt LS-DYNA ALE usages, Structured ALE solver introduced a new, user-friendly, streamlined three-step setup. We hope this effort could help users, new or old, to perform their work more efficiently and smoothly.

Providing engineering services to the composites industry since 1970. During this time, we have participated in numerous programs that demonstrate our ability to perform advanced composite design, analysis and testing; provide overall program management; work in a team environment; and transition new product development to the military and commercial sectors.

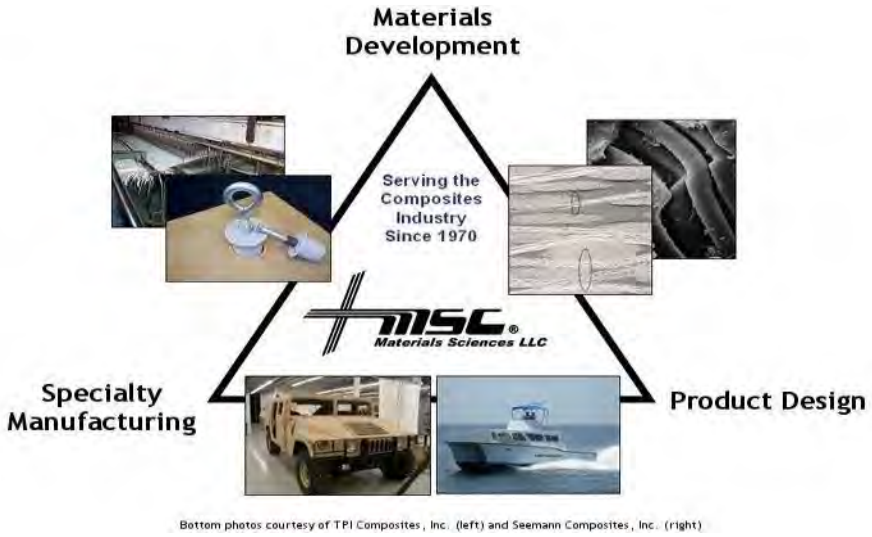

MSC/LS-DYNA Composite Software and Database

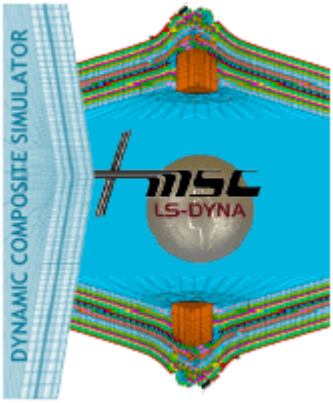

Materials Sciences Corporation (MSC) and Livermore Software Technology Corporation (LSTC) announce the Dynamic Composite Simulator module of LS-DYNA.

This enhancement to LS-DYNA, known as MAT161/162, enables the most effective and accurate dynamic progressive failure modeling of composite structures.

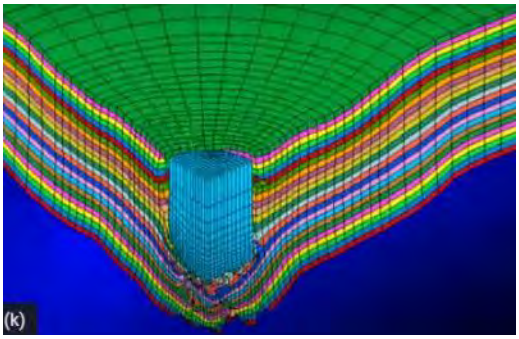

Dyna Fact Sheet (PDF)

Pricing and Contact:

- Types of licenses include: Educational, Commercial, and 30-Day Trial (US only).
- MAT161/162 annual licenses start at $1725 for commmercial use and $175 for educational. (New pricing effective 2017. Contact us for details.)
- Licenses include User's Manual and Technical Support (maintenance, support and updates for time duration of license).
- Please call 215-542-8400 or email dyna_161@materials-sciences.com for more information.

This helps our clients avoid pitfalls, and make exceptionally rapid technological progress. The same broad reach allows us the opportunity to interact with, and evaluate a wide range of suppliers.

Oasys Ltd is the software house of Arup and distributor of the LS-DYNA software in the UK, India and China. We develop the Oasys Suite of pre- and post-processing software for use with LS-DYNA.

Oasys LS-DYNA Virtual Update Meeting 2021

For the first time ever, we'll be bringing together Oasys LS-DYNA users from across the globe to join a free, online event providing updates about developments in the Oasys LS-DYNA Environment software.

Register here

Get ready for Oasys Suite 18.0

Version 18.0 of the software will include a number of new features to make it easier to use, increase performance, and better automate your processes. This latest version of the software will use the LM-X licensing platform to provide an increased level of license security. FLEXlm is not used for Oasys licensing from version 18.0 onwards.

To ensure you're ready to enjoy all the great features Oasys Suite 18.0 will bring, we recommend you update all your Oasys Suite license servers and files as soon as possible.

For more information view our website.

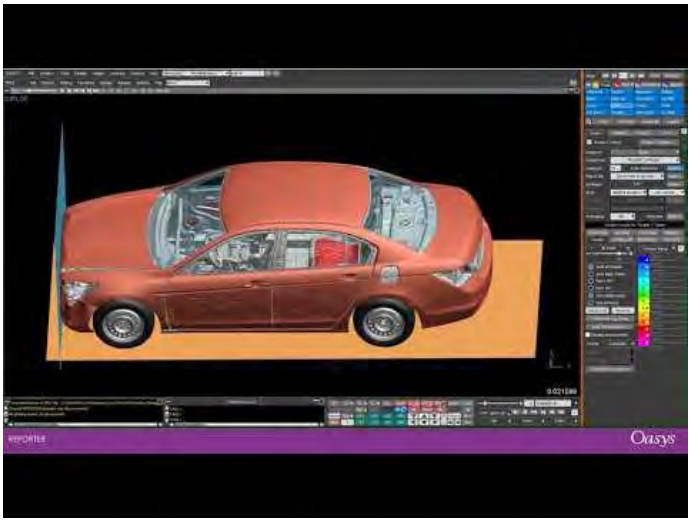

Top Tip video: Did you know?

Oasys REPORTER can link with your D3PLOT and T/HIS sessions to help you easily create reports with analysis results.

← Click on the image to watch.

Annual GHBMC Users' Workshop

27th April 2021

The annual GHBMC Users' Workshop is a free virtual event. As part of this workshop, Gavin Newlands will present on how Oasys PRIMER's positioning tools can be used to achieve realistic articulation and positioning of Human Body Models.

The talk will also cover the model trees which are now available in Oasys PRIMER to help you easily and accurately position the industry-leading GHBMC models.

Please visit our Oasys HBM webpage to find out more about the GHBMC positioning trees we support in Oasys PRIMER.

You can register for the event via the Elemance website, distributor of the GHBMC family of virtual HBMs, using the link below.

Register for the workshop here.

Predictive Engineering

www.predictiveengineering.com

Predictive Engineering provides FEA and CFD consulting services, software, training and support to a broad range of companies.

FINITE ELEMENT ANALYSIS
Predictive Engineering

LS-DYNA has been one of Predictive's core analysis tools pretty much since we got started in 1995. It is an amazing numerical workhorse from the basic linear mechanics (think ANSYS or Nastran) to simulating well nigh the impossible. At least that is the way I feel at times when the model is not solving and spitting out arcane error messages and I'm basically questioning my sanity for accepting this project from hell that has a deadline at the end of the week. Which brings me to my favorite project management image – "trough of despair followed by wiggles of false hope then crash of ineptitude and finally the promised land" but I'll leave that for another blog.

Predictive Engineering – Western States ANSYS LS-DYNA Distributor

For now, let's talk about those free coffee cups. Predictive is now the western states distributor of ANSYS LS-DYNA and provides complete sales, training and services for ANSYS LS-DYNA clients in this region. It is a continuation of our prior setup with LSTC (now ANSYS LST) with the addition of Predictive's ability to offer ANSYS Workbench with LS-DYNA and other ANSYS software tools. So where's my free coffee cup? If you are a current Predictive ANSYS LS-DYNA client, we'll be shipping'em out to you at the end of February and for our new client's – just send us an email or give us a call.

View our portfolio

FEA, CFD and LS-DYNA consulting projects

Composite Engineering	Nonlinear Dynamics	Aerospace
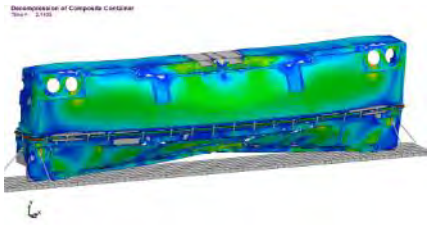	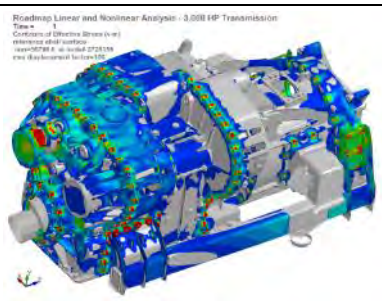	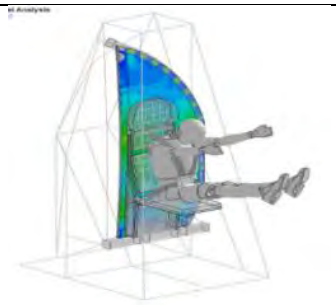

Contact:

Address:
2512 SE 25th Ave
Suite 205
Portland, Oregon 97202
USA

Phone:
503-206-5571
Fax:
866-215-1220
E-mail:
sales@predictiveengineering.com

Offering industry-leading software platforms and hardware infrastructure for companies to perform scientific and engineering simulations. Providing simulation platforms that empower engineers, scientists, developers, and CIO and IT professionals to design innovative products, develop robust applications, and transform IT into unified, agile environments.

4 Reasons Why Others are Adopting Cloud HPC and EDA Should Too!

March 11, 2021
Engineering, English, Semiconductor
Tanner Ham

With the complexity of transistors at an all-time high and growing foundry rule decks, fabless companies consistently find themselves in a game of catch-up. Semiconductor designs require additional compute resources to maintain speed and quality of development. But deploying new infrastructures at this current speed is a tall order for IT professionals tasked with supporting development and verification teams. When these resources can't keep up, engineers become compute constrained rather than compute empowered.

The semiconductor industry is not alone in the struggle to adopt new technologies that can accelerate the pace of science and engineering breakthroughs. For that reason, cloud solutions are increasingly being implemented to empower R&D in a way never before seen. Breakthroughs in aerospace design, new drugs and vaccines, alternative energy solutions, and much more are now being realized on cloud or cloud HPC infrastructures. Because of security and IP concerns, EDA companies have primarily maintained on-premise data centers for their computing needs. However, that preference is changing due to manufacturers such as TSMC endorsing cloud. The industry has also seen a rise in startups entering the industry that do not have the infrastructure of their own and are turning to the cloud to compete.

So let's look at the main benefits of expanding EDA to a cloud HPC environment.

Security

As companies look to move workloads to the cloud, the primary area of focus is how to protect sensitive information and IP. Recent research by Cloud Vision states, two-thirds of companies consider this the main roadblock in adopting cloud. In light of this, major cloud providers have put substantial focus and investment to reduce risks and safeguard datacenters from any breach. As you can imagine, with companies like AWS, Microsoft, and Google, no expense is spared to ensure they deliver a secure environment. As proof of these security measures, the public cloud will experience 60% fewer security incidents compared to typical data centers this year. For organizations that require full-stack compliance and security, platforms such as Rescale cover end-to-end workflows across the hardware and software layers with the highest of industry standards. Even going as far as obtaining industry-leading certifications to meet the strictest compliance requirements.

Agility

Never in our history has technological agility been more important than 2020. Facing a pandemic was the ultimate test of our systems and most companies found themselves not prepared. Being cut off from typical on-premise infrastructure caused delays across the industry. VPNs became overwhelmed as engineers struggled to access the data and resources needed to continue development and run verification. The need to enable remote teams is not the only consideration. Systems need to have the flexibility to scale with phases of projects and production deadlines. For these reasons, cloud far outperforms traditional infrastructures. It's accessible anywhere you can find a wifi connection and compute resources scale as needed. The Rescale platform also offers remote desktop solutions and a wide variety of admin controls over budgets and permissions to keep operations running smoothly. With the stability and options of a multi-cloud infrastructure and a variety of core types available on the platform, users can match the ideal core type to their workload and be confident in the stability of the infrastructure with a service level agreement that their job will run.

Impact and Productivity

Enabling engineers to focus on design means better products at a quicker pace. IT leaders need to look at the ways in which engineers are distracted or slowed from their core responsibilities. Companies spend top dollar to secure engineering expertise and talent and they should be working on the portion of the business where they will make the biggest impact. Distractions can come in the form of queues, slow workflows, license issues, and more. Rescale looks to solve these issues with an intelligent control plane and full-stack approach. Having an intelligent control plane for both local and cloud hardware allows R&D the ability to divert workloads to the best infrastructure based on performance and cost. A simple user interface with robust automation allows them to easily set up runs without relying on IT. And if they do come across a challenge, the Rescale support team is stacked with HPC and simulation experts that average a 15 min response time. All of this combines to allow engineers to be hyper-focused on what they do best.

Speed to Market

A major component of gaining a competitive advantage is to be first to market with a new product. This allows you to gain brand recognition, build customer loyalty, and secure market share before competitors are even in play. A cloud approach enables semiconductor companies to dial up the number of iterations and accelerate speed to answer. Additionally, verification is expedited with virtually unlimited resources available. When coupled with automated workflows, templates, and continuous optimization from the Rescale platform, companies can make substantial improvements.

pSemi used Rescale to substantially speed up their development process, "We were able to use Rescale's cloud platform to highly parallelize our simulations and bring the simulation time down from 7 days to 15 hours. We've demonstrated a 10x speed improvement on numerous occasions in our EM simulations using Rescale…"

The next wave of semiconductor advancements will be powered by the cloud. The foundries have already started to adopt the technology. It is poised to revolutionize the industry by empowering engineers like never before and reaching new levels of performance and efficiency.

LS-DYNA China, as the master distributor in China authorized by LST, an Ansys company, is fully responsible for the sales, marketing, technical support and engineering consulting services of LS-DYNA in China.

Shanghai Fangkun Software Technology Ltd

Shanghai Fangkun Software Technology Ltd. was authorized by ANSYS Inc as the domestic master distributor of LS-DYNA software. Shanghai Fangkun is fully responsible for domestic sales, marketing, technical support of LS-DYNA. By integrating and managing a wide range of resources such as LS-DYNA agents and partners, Shanghai Fangkun is focus on providing a strong technical support for domestic LS-DYNA users, and help customers to effectively use LS-DYNA software for product design and development.

Based on the strong technical support and developing capability from ANSYS Inc, Shanghai Fangkun attracts a group of top LS-DYNA application engineers and commit to provide LS-DYNA technical support in the automotive industry, electronics industry, rock-soil, aerospace, general machinery and other industries. Shanghai Fangkun devotes to providing all products of LSTC including LS-DYNA, LS-OPT, LS-PREPOST, LS-TASC and LSTC FEA models (dummies model, pedestrian model, etc).

In the meantime, Shanghai Fangkun also relies on strong technical support of ANSYS Inc and will focus on secondary development and process customization of LS-DYNA and its application process. In view of domestic users customization requirement, Shanghai Fangkun will concentrate on customizing custom interface based on LS-PREPOST processing platform, to adjust, standardize and analyzes specific process, improve the efficiency in application, reduce human error, accumulate experience of engineering application, improve customer R&D and competition capabilities.

Shanghai Fangkun will keep mission firmly in mind, devote to improving user satisfaction of LS-DYNA and providing high-quality technical support and engineering consulting services for users.

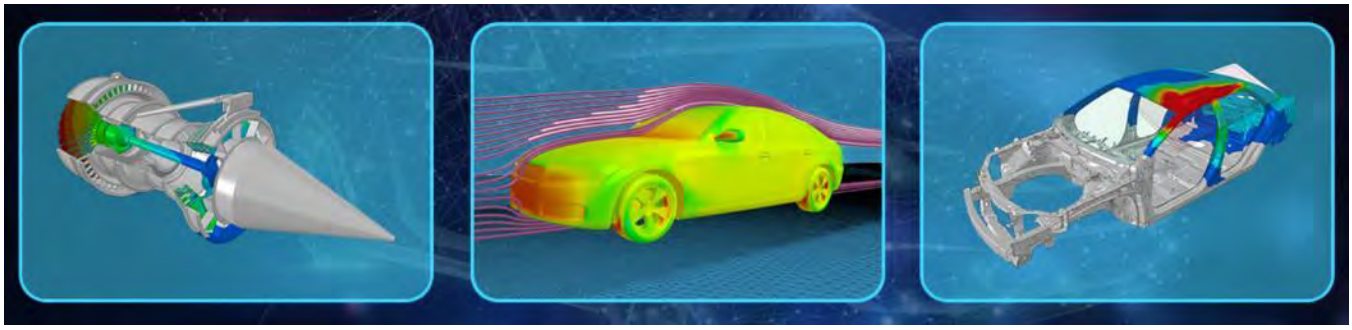

Contacts

Address: Room 2219, Building No.1, Global Creative Center, Lane 166, Minhong Road, Minhang District, Shanghai
Postcode： 201102 **Tel：** 4008533856 021-61261195
Sales Email： sales@lsdyna-china.com Technical Support Email：support@lsdyna-china.com

LS-DYNA Training Plan in 2021

Shanghai Fangkun has successfully held several series of LS-DYNA related webinars and training courses in 2020 and received much attention and feedback. Now Shanghai Fangkun release the training plan for 2021 as shown in the following table. Please follow us official Wechat "LSDYNA" to get latest information. All LS-DYNA users and those who interested in are welcome to attend. If you have any questions, please contact email **training@lsdyna-China.com, or dial 021-61261195, 4008533856.**

Date	Topic	Duration
Jan.	LS-DYNA Basic Training	2 days
Feb.	Introduction to LS-PrePost	4-8 hours
Feb.	Introduction to LS-Form & Stamp forming	4-8 hours
Mar	Crash & Safety analysis in LS-DYNA	2 days
Mar	Introduction to LS-Form & Stamp forming	4-8 hours
Apr	GISSMO failure model theory and application of LS-DYNA	4-8 hours
Apr	Simulation of battery crush and nail penetration in multiphysical field with LS-DYNA	4-8 hours
May	Concrete material model in LS-DYNA	2-4 hours
May	Introduction to S-ALE	4-8 hours
Jun	Drop analysis in LS-DYNA	4-8 hours
Jun	Introduction to Contact in LS-DYNA	4-8 hours
Jul	Introduction to EM in LS-DYNA	4-8 hours
Jul	Introduction to LS-OPT	4-8 hours
Aug	ICFD analysis in LS-DYNA	2-4 hours
Aug	LS-DYNA Basic Training	4-8 hours
Sep	Implicit analysis in LS-DYNA	4-8 hours
Sep	CESE analysis in LS-DYNA	2-4 hours
Oct	LS-DYNA application in constranit system	4-8 hours
Oct	Meshfree,SPG and Advanced finite element analysis in LS-DYNA	4-8 hours
Nov	LS-DYNA composite material model training	4-8 hours
Nov	LS-DYNA Thermal-structural-Coupling Analysis	4-8 hours
Dec	LS-DYNA Welding Analysis	4-8 hours
Dec	NVH, Frequency domain and fatigue in LS-DYNA	4-8 hours

Shanghai Fangkun Software Technology Ltd. was authorized by ANSYS Inc as the domestic master distributor of LS-DYNA software and will keep mission firmly in mind, devote to improving user satisfaction of LS-DYNA and providing high-quality technical support and engineering consulting services for users.

CAE software sale & customer support, initial launch-up support, periodic on-site support. Engineering Services. Timely solutions, rapid problem set up, expert analysis, material property test Tension test, compression test, high-speed tension test and viscoelasticitiy test for plastic, rubber or foam materials. We verify the material property by LS-DYNA calculations before delivery.

TERRABYTE Co.,Ltd.
Customer Satisfaction by Computer Solution & Computer Simulation

CAE consulting - Software selection, CAE software sale & customer support , initial launch-up support, periodic on-site support.

Engineering Services - Timely solutions, rapid problem set up, expert analysis - all with our Engineering Services. Terrabyte can provide you with a complete solution to your problem; can provide you all the tools for you to obtain the solution, or offer any intermediate level of support and software.

FE analysis

- LS-DYNA is a general-purpose FE program capable of simulating complex real world problems. It is used by the automobile, aerospace, construction, military, manufacturing and bioengineering industries.
- ACS SASSI is a state-of-the-art highly specialized finite element computer code for performing 3D nonlinear soil-structure interaction analyses for shallow, embedded, deeply embedded and buried structures under coherent and incoherent earthquake ground motions.

CFD analysis

- AMI CFD software calculates aerodynamics, hydrodynamics, propulsion and aero elasticity which covers from concept design stage of aerocraft to detailed design, test flight and accident analysis.

EM analysis

- JMAG is a comprehensive software suite for electromechanical equipment design and development. Powerful simulation and analysis technologies provide a new standard in performance and quality for product design.

Metal sheet

- JSTAMP is an integrated forming simulation system for virtual tool shop based on IT environment. JSTAMP is widely used in many companies, mainly automobile companies and suppliers, electronics, and steel/iron companies in Japan.

Pre/ Post

- **PreSys** is an engineering simulation solution for FE model development. It offers an intuitive user interface with many streamlined functions, allowing fewer operation steps with a minimum amount of data entry.
- **JVISION** - Multipurpose pre/post-processor for FE solver. It has tight interface with LS-DYNA. Users can obtain both load reduction for analysis work and model quality improvements.

Biomechanics

- **The AnyBody Modeling System™** is a software system for simulating the mechanics of the live human body working in concert with its environment.




- New 2021 Jeep® Gladiator Texas Trail debuts featuring 17-inch Mid-Gloss Black aluminum wheels, 32-inch mud-terrain tires and Trailer Tow Group
- Jeep Gladiator Texas Trail's rugged exterior features unique Texas Trail hood and tailgate decals with the year 1836 as a nod to the Texas Declaration of Independence
- Standard features include side steps, Trailer Tow Group, black hardtop, black leather seats embossed with the Texas Trail graphic and Technology Group with 7-inch radio and convenience group
- Industry-exclusive Jeep Badge of Honor mobile app now features two trails in Texas
- Jeep Wave® customer service program comes standard with Gladiator Texas Trail
- Jeep Gladiator Texas Trail is available now at dealers in the state of Texas and has a starting MSRP of $40,435

April 12, 2021 , Auburn Hills, Mich. - The Jeep® brand is blazing new trails in Texas, the largest truck market in the country, by introducing the new 2021 Gladiator Texas Trail. Based on the Gladiator Sport S trim, the Texas Trail is launching exclusively for the state of Texas and delivers a new level of personalized content for a distinct appearance combined with legendary Jeep 4x4 capability.

"The Jeep brand recognizes that Texas and America's southwest are the center of the truck universe," said Jim Morrison, Vice President Jeep Brand North America. "Special editions allow us to connect with our passionate customers, and the Jeep Gladiator

2021 Jeep® Gladiator Texas Trail Celebrates Largest Truck Market, Jeep Badge of Honor Program Adds Two Texas Trails

Texas Trail further broadens the appeal of the most capable Jeep pickup yet."

The 2021 Jeep Gladiator Texas Trail also celebrates the addition of two Texas trails to the Jeep Badge of Honor program. The industry-exclusive Jeep Badge of Honor mobile app allows off-road enthusiasts to conquer trails and earn unique trail badges for their Jeep vehicles. Texas is now home to two Badge of Honor trails, including Black Gap 4x4 trail in Big Bend National Park and Northwest OHV Park in Bridgeport, Texas.

The 2021 Jeep Gladiator Texas Trail is available now at dealers in the state of Texas.

Jeep Gladiator Texas Trail

Bolstering the 2021 Jeep Gladiator lineup, the new Texas Trail marks the first time Jeep is offering a truck that pays homage to the largest truck market in the country: Texas. The Gladiator Texas Trail features 17-inch Mid-Gloss Black Aluminum wheels wrapped in 32-inch mud-terrain tires. These features, combined with the Jeep Command-Trac 4x4 part-time, two-speed transfer case with a 2.72:1 low-range gear ratio, enhance the Gladiator Texas Trail's off-road capability.

This added capability is highlighted with a rugged exterior. The unique Texas Trail hood and tailgate decals include the year 1836 as a nod to the Texas Declaration of Independence. The Sport S-based Gladiator Texas Trail also includes standard side steps, Trailer Tow Group, black hardtop, black leather seats embossed with the Texas Trail graphic and Technology Group with 7-inch radio and Convenience Group.

The 2021 Jeep Gladiator, engineered from the ground up to be the most off-road capable Jeep truck ever, builds on a rich heritage of tough, dependable Jeep trucks with an unmatched combination of rugged utility, authentic Jeep design, open-air freedom, clever functionality and versatility.

Available with the new 3.0-liter EcoDiesel V-6 engine, rated at 260 horsepower and 442 lb.-ft. of torque, or the 3.6-liter Pentastar V-6 engine, rated at 285 horsepower and 260 lb.-ft. of torque, and a versatile cargo box, Gladiator is built to handle the demands of an active lifestyle while delivering an open-air driving experience in a design that is unmistakably Jeep. Combining traditional Jeep attributes with strong truck credentials, the Jeep Gladiator is a unique vehicle capable of taking passengers and cargo anywhere.

Jeep Gladiator Texas Trail is Trail Rated with a badge indicating that the vehicle is designed to perform in a variety of challenging off-road conditions, identified by five key consumer-oriented performance categories: traction, ground clearance, maneuverability, articulation and water fording.

The Gladiator Texas Trail is available in 10 colors: black, white, Snazzberry, Granite Crystal, Sarge, Nacho, Hydro Blue, Firecracker Red, Billet Silver and Sting-Gray.

The 2021 Jeep Gladiator Texas Trail has a starting MSRP of $40,435 (plus $1,495 destination) and is currently available at Texas dealers.

Jeep Wave® Customer Care Program

Jeep Wave is a premium owner loyalty program filled with benefits and exclusive perks created to give Jeep owners the utmost care and dedicated 24/7 support. The Jeep Wave customer service program is available to the entire 2021 model-year Jeep brand lineup.

Jeep Wave program highlights include:

- Three years of worry-free maintenance at Jeep dealerships, including oil changes and tire rotations
- 24/7 support via phone or online chat
- Trip interruption and first-day loaner coverage
- VIP access to select, exclusive Jeep events

Jeep Brand

Built on 80 years of legendary heritage, Jeep is the authentic SUV with capability, craftsmanship and versatility for people who seek extraordinary journeys. The Jeep brand delivers an open invitation to live life to the fullest by offering a full line of vehicles that continue to provide owners with a sense of security to handle any journey with confidence. Jeep Wave, a premium owner loyalty and customer care program that is available to the entire Jeep lineup, is filled with benefits and exclusive perks to deliver Jeep owners the utmost care and dedicated 24/7 support.

The Jeep vehicle lineup consists of the Cherokee, Compass, Gladiator, Grand Cherokee, Renegade and Wrangler. To meet consumer demand around the world, all Jeep models sold outside North America are available in both left- and right-hand drive configurations and with gasoline and diesel powertrain options. Jeep is part of the portfolio of brands offered by leading global automaker and mobility provider Stellantis. For more information regarding Stellantis (NYSE: STLA), please visit www.stellantis.com.

Read from website

LS-DYNA - Resource Links

LS-DYNA Multiphysics YouTube

https://www.youtube.com/user/980LsDyna

FAQ LSTC

ftp.lstc.com/outgoing/support/FAQ

LS-DYNA Support Site

www.dynasupport.com

LS-OPT & LS-TaSC

www.lsoptsupport.com

LS-DYNA EXAMPLES

www.dynaexamples.com

LS-DYNA CONFERENCE PUBLICATIONS

www.dynalook.com

ATD –DUMMY MODELS

www.dummymodels.com

LSTC ATD MODELS

www.lstc.com/models www.lstc.com/products/models/mailinglist

AEROSPACE WORKING GROUP

http://awg.lstc.com

Training - Webinars

Participant's Training Classes

Webinars

Info Days

Class Directory

Directory

ANSYS	https://www.ansys.com/services/training-center
BETA CAE Systems	www.beta-cae.com/training.htm
DYNAmore	www.dynamore.de/en/training/seminars
Dynardo	http://www.dynardo.de/en/wost.html
ESI-Group	https://myesi.esi-group.com/trainings/schedules
ETA	http://www.eta.com/training
KOSTECH	www.kostech.co.kr
ANSYS LST	www.lstc.com/training
LS-DYNA OnLine - (Al Tabiei)	www.LSDYNA-ONLINE.COM
OASYS	www.oasys-software.com/training-courses
Predictive Engineering	www.predictiveengineering.com/support-and-training/ls-dyna-training

LS-DYNA Online Training

LS-DYNA LIVE ONLINE TRAINING & CONSULTING SERVICES

Lsdyna online was created by the LSTC instructor after 25 years of teaching various LS-DYNA courses for LSTC nationally and internationally (more than 20 countries). The online company was established in 2012 and we have been providing many live interactive courses to many companies and organizations. We do consulting work in addition to instructions. Here are some courses, for full list see our webpage.

About Tabiei

Dr. Al Tabiei has been a consultant on the use of large scale finite element simulation for more than 25 years to more than 80 large and small companies and government labs in the US and abroad. He was the director of the Center of Excellence in DYNA3D Analysis at the University of Cincinnati (1997-2001). He has more than 150 journal, refereed reports, and conferences papers

He lectured at nearly 20 countries. He also did code development for LSTC. The instructor has developed and implemented many material models in LS-DYNA. Composite Shell element for composite materials and various other development in the code. He was consultant to the US government for several years on the use of simulation for home land security problems. He has served as a Subject Matter Expert (SME) for the government for more than 20 years. He was also on a NASA team for the return to the moon program to investigate different landing scenarios (2006-2010).

Electrochemical-Thermal-Mechanical coupling of Lithium-Ion Battery Model in LS-DYNA

Kyoungsu Im[1], Jaeyoung Lim[2], Kyu-Jin Lee[3], Z.-C. Zhang[1], and Grant Cook, Jr.[1]

[1]*Livermore Software Technology, an ANSYS Company, Livermore, CA 94551, USA*
[2]*Hyundai Motor Group R&D Division, Gyeonggi-do, 18280, KOREA*
[3]*Dept. of Mech. Eng., Myongji University, Yongin 449-728, KOREA*

Abstract

In this paper, we report a new development of battery-thermal-structure-interaction (BTSI) based on previously developed electrochemical Lithium-Ion models: i) a single insertion lithium metal model, and ii) a dual insertion composite model. In 10 cells of a lithium ion battery stack, each cell consists of Graphite(LiC_6) anode/Separator/high performance layered LMO($LiMn_2O_4$) or NCM($LiNi_{1/3}Co_{1/3}Mn_{1/3}O_2$) cathode, which has been strongly proposed as a candidate for automotive batteries because of its high capacity, thermal stability, and low volume change rate (cycle performance). For the thermal-mechanical analysis, each layer in a cell and outside case are modeled corresponding to their material properties. Then, a rigid ball impacts center top position of the cell stack in order to investgate the thermal and mechanical responses of a lithium ion battery stack. To see the cell responses in different state of charge(SOC), we selected the first 20 second of the discharging processes. The results show that after the ball impact the cell stack, then the mechanical deformation started and 6 seconds after the ball compressed, a strong hot spot developed inside cell stack and the temperature increaed exponentially over the melting point of the lithium, 453K. Although we demonstrated a simple impact problem to show how to simulate the electrochemical-thermal-mechanical problem, the current solver can be used to solve more practical problems such as a cellular phone drop test, notebook battery impacting test, and even deformation test of the scaled-up electric vehicle(EV) battery pack.

Introduction

The research and technology of lithium-ion batteries(LIB) has grown extensively since Sony first introduced it on the market in 1991. Such a technology nowadays becomes a stand power source in a broad range of indispensable life equipment including cell-phones, laptop computers, and electric vehicles(EV). The most comparative advantages of LIB from the conventional batteries include [1]: i) efficient rate and high power discharge capability, ii) distinguished specific energy and its energy density, iii) stable operation with a wide range of temperature, iv) small discharge rate and long life cycle, and so on. Such excellent features now make it possible to replace EV batteries gradually. For example, the Nissan Leaf and most of Tesla Motors's models are widely known commercialized EVs that contain LIBs. Generally, the battery pack in EV are made up of thousands of cells so that it can be possible to accelerate the car from 0 to 60 miles per hour within a few seconds. Furthermore, comparatively long range driving can also be possible with with increasing power density of LIB.

Although LIB has many excellent features and it has been proven that LIBs are safe enough to the commercial EV, as more energy is stored, more possible dangers for the safety arise. One of the most dangerous and extreme issues with LIB safety is the possibility of thermal runaway[2]. In fact, accidents due to battery malfunctions have been reported. For example, a Tesla model S caught fire started in battery after the EV hit metal debris on a highway[3]. Therefore, it is inevitable that more improvement in the

area of the thermal safety is required [2]. In addition, the demand for improvement from thermal degradation in high temperature situations is undeniably required [1].

Chen and Evans[4,5] extended thermal modeling of lithium/polymer battery model to electric vehicle(EV) application using a scaled-up 2D and 3D heat condition model for the serially connected unit cells and parallel connected cell stacks. Without directly calculate the heat generations from LIB models, they used the theoretical capacity equations which fitted by using empirical parameters for discharge and charge processes. The main messages from their simulation shown that the thermal management may not be serious for batteries under low discharge rate, but in the case of high discharge rate, the temperature will be remarkably increased if the thickness of a cell stack exceed a certain threshold value.

The important attempt at predicting the thermal behavior of the lithium/polymer battery using 1D LIB model was made by Carolyn R. Pals and John Newman[6] who conducted simulations of two different models: a single cell, and a cell stack. In a single cell model, they examined that how cell performance varies with operating temperature for both adiabatic and isothermal discharge. It was shown that cells operating at lower temperature have a lower cell potential and reach their cutoff potential sooner, and at a lower value of active material utilization than cells operating at a higher temperature due to variation with temperature of the salt diffusion coefficient and the ionic conductivity. Using the cell stack model, they demonstrated how the temperature varies in a cell stack depending on thickness and heat transfer conditions and concluded that heat was generated at lower rates in higher temperature areas of the stack , and at higher rates in lower temperature areas of the stack, with such nonuniform heat generation rate make the temperature profiles in the cell stack flatten.

Later on, Song and Evans[7] improved their thermal model for lithium polymer batteries by using electrochemical-thermal modeling. Based on the author's knowledge, this is the first mathematical approach that the electrochemical phenomena is coupled simultaneously with 2D heat conduction. By using Doyle's[8, 9] 1D a single insertion model, they compared to their results to the experimental data for various cell voltages as a function of discharge capacity. Although their results showed some discrepancies, they concluded that their results are in reasonable agreement with the experimental data.

However, there is no model existing for the treatment of the electrochemical-thermal-mechanical(ECTM) phenomena simultaneously. In the present paper, we report the recent development of an ECTM coupled LIB model in LS-DYNA®. At a given time step, the heat generation is determined in each structural element that is considered as a 1D electrochemical cell (inside the battery). Based on such heat generations, the thermal solver computes the temperature of cell elements in a 3D computational domain with the electrochemical parameters of each cell. Finally, the thermal solver communicates with mechanical solver by exchanging thermal properties and works done by mechanical solver, which the mechanical properties of the LIB are required and are taken into account, including Yong's modules, stress, and Poisson's ratio[10]. When coupled this way, the mechanical solver transfers its deformation coordinates to the electrochemical LIB solver. It should be noted that the present model is based on the thermodynamics, kinetics, and concentrated solution transport theories in pores of composite electrodes and is intended to assist users in tackling problems ranging from the fundamental battery cell physics to very complex situations such as EV crush models. To this end, we have designed detailed keywords for the electrodes, electrolytes, transport material properties, and even thermal-mechanical couplings for such applications

Modeling of the Lithium Ion Battery

A full understanding of the multi-physics involved in LIB models is necessary for correct simulation of these models. This includes material transport, thermodynamics, and kinetics in the porous electrode. Porous media are normally used with concentrated electrolytes. Such a theory was first pioneered by Newman and Tiedman[11]. In their porous electrode theory, the properties determining the battery performance were averaged over a small volume in all dimensions of the electrode without specifying the exact positions, shapes of all electrode particles, and the exact pores in each electrode. Thus, the porous electrode is

considered as the superposition of all materials coexisting in the active insertion material, filler, and electrolyte at every point of the geometry. In what follows, we will first review and construct the transport model equations based on the concentrated solution theory, the potential equations with thermodynamics, equations for electrochemical kinetics and the current balance, and then, the energy balance equations including heat generation in a single cell and scaled-up energy equation.

Transport

The driving force acts on species *i*, and causes it to move with respect to the surrounding fluid. This is determined by the difference of the electrochemical potential multiplied by species concentration, which is in turn given as the Stefan-Maxwell multicomponent diffusion equation [12,13]:

$$c_i \nabla \mu_i = \sum_j K_{ij} \left(\mathbf{v}_j - \mathbf{v}_i \right) = RT \sum_j \frac{c_i c_j}{c_T D_{ij}} \left(\mathbf{v}_j - \mathbf{v}_i \right) \quad (1)$$

where μ_i is the electrochemical potential of species *i*, K_{ij} are friction coefficients, and $\mathbf{v}_i$ is the velocity of species *i*. With the selection of a reference velocity, which is chosen for the solvent, these equations can be inverted to yield flux equations for the anion and cation in a binary electrolyte,

$$c_+ \nabla \mu_+ = K_{0+} \left(\mathbf{v}_0 - \mathbf{v}_+ \right) + K_{+-} \left(\mathbf{v}_- - \mathbf{v}_+ \right) \quad (2a)$$

$$c_- \nabla \mu_- = K_{0-} \left(\mathbf{v}_0 - \mathbf{v}_- \right) + K_{+-} \left(\mathbf{v}_+ - \mathbf{v}_- \right) \quad (2b)$$

since the flux density of species *i* is given by

$$N_i = c_i \mathbf{v}_i \quad (3)$$

and the current density in an electrolyte solution given by

$$i = F \sum_i z_i N_i \quad (4)$$

Then, the equation can be rearranged as,

$$N_+ = c_+ \mathbf{v}_+ = -\frac{\nu_+ D c_T}{\nu RT c_0} c \nabla \mu_e + \frac{i_2 t_+^0}{z_+ F} + c_+ \mathbf{v}_0 \quad (5a)$$

$$N_- = c_- \mathbf{v}_- = -\frac{\nu_- D c_T}{\nu RT c_0} c \nabla \mu_e + \frac{i_2 t_-^0}{z_- F} + c_- \mathbf{v}_0 \quad (5b)$$

where $c = c_+ / \nu_+ = c_- / \nu_-$, $\nu = \nu_+ + \nu_-$, and $\mu_e = \nu_+ \mu_+ + \nu_- \mu_- = \mu^0{}_e + \nu RT \ln(\gamma_\pm m)$, with $m = c/c_0 M_0$. The diffusion coefficient of electrolyte and the transference number with respect to the solvent are related to the diffusion coefficients by

$$D = \frac{D_{0+} D_{0-} \left(z_+ - z_- \right)}{z_+ D_{0+} - z_- D_{0-}} , \quad (6)$$

and

$$t_+^0 = 1 - t_-^0 = \frac{z_+ D_{0+}}{z_+ D_{0+} - z_- D_{0-}} \quad (7)$$

From porous electrode theory, a differential material balance can be averaged over the volume of the pores in an element of the electrode, and the surface integrals can be introduced by means of the divergence theorem and the final mass balance for species *i* [14]:

$$\varepsilon \frac{\partial c_i}{\partial t} = -\nabla \cdot \mathbf{N}_i + a j_{in} \quad (8)$$

where c_i is an average over the volume of the solution in the pores, j_{in} is an average over the interfacial area between the matrix and the pore solution, and N_i is an average over a cross section through the electrode, cutting matrix and pore. It should note that three different averages are applied to derive the mass transport, Eq.(8) in porous media.

The diffusion coefficient of the salt which is the property commonly measured for a binary electrolyte can be related to the diffusion coefficient of the electrolyte by,

$$\mathrm{D} = D \frac{c_T}{c_0}\left(1 + \frac{d \ln \gamma_{\pm}}{d \ln m}\right) \quad (9)$$

where $\gamma_{\pm}$ is the mean molal activity coefficient and m is the molality. The gradient of chemical potential can be expressed in terms of the gradient of concentration:

$$\frac{D}{\nu RT}\frac{c_T}{c_0} c \nabla \mu_e = D\left(1 - \frac{d \ln c_0}{d \ln c}\right)\nabla c \quad (10)$$

Using the above relation, the flux of species i can be expressed as,

$$N_i = -\nu_i \left(1 - \frac{d \ln c_0}{d \ln c}\right) D \nabla c + \frac{i_2 t_i^0}{z_i F} + c_i \mathbf{v}_0 \quad (11)$$

Detailed derivation of Eq.(10) (or from Eq. (5) to Eq. (11)) can be found in Appendix A[15]. Finally, by inserting equation (11) into equation (8), the mass transfer equation in porous media can be derived as,

$$\varepsilon \frac{\partial c}{\partial t} + \nabla \cdot (c \mathbf{v}_0) = \nabla \cdot \left[\varepsilon D\left(1 - \frac{d \ln c_0}{d \ln c}\right)\right]\nabla c - \frac{\nabla \cdot \left(i_2 t_+^0\right)}{z_+ \nu_+ F} + a j_+ \quad (12)$$

Convection in the electrolyte is usually negligible and $z_+\nu_+$ is 1 for most salts used in LIBs. The boundary condition on the salt concentration at a lithium foil electrode (a single insertion model) is found by setting the anion flux to zero:

$$\varepsilon \left.\frac{\partial c}{\partial x}\right|_{x=0} = -\frac{I\left(1 - t_+^0\right)}{FD} \quad (13)$$

At the boundary between the positive electrode and current collector, the flux of ions is equal to zero, and all of the current is carried by electrons, so the salt concentration and the current density of electrolytes is set to zero:

$$\nabla c = 0 \text{ and } \mathbf{i}_2 = 0, \text{ at x=XL} \quad (14)$$

For the dual insertion model, the boundary conditions on negative electrode and current collector are analogous to those of the positive case. The porous solid phase in most LIBs contains particles which can be modeled as spheres. If volume changes in the solid are negligible, the mass balance reduces to,

$$\frac{\partial c_s}{\partial t} = \frac{1}{r^2}\frac{\partial}{\partial r}\left(D_s r^2 \frac{\partial c_s}{\partial r} \right) \quad (15a)$$

with the boundary conditions,

$$\left.\frac{\partial c}{\partial r}\right|_{r=0} = 0, \text{ and } -D_s \left.\frac{\partial c}{\partial r}\right|_{r=R} = j_{Li^+} \quad (15b)$$

and initial condition,

$$c_s\left(t=0, r\right) = c_s^0 \quad (15c)$$

The second boundary condition is constructed by relating the pore wall flux across the interface with the rate of transport of lithium ions into the solid phase. Under the diffusion process, the superficial area per unit volume of the porous electrode is related to the particle radius:

$$a = \frac{3\left(1-\varepsilon\right)}{R_s} \quad (16)$$

Potential

In LIB model, the gradient of the potential in the solution is to be defined with respect to a lithium reference electrode in solution [14]:

$$\nabla\Phi_2 = -\frac{i_2}{\kappa} + \frac{RT}{F}\left(1-t_+^0\right)\cdot\left(1+\frac{d\ln f_A}{d\ln c}\right)\nabla\ln c \quad (17)$$

The second term on the righthand side accounts for concentration overpotential. In porous media, the conductivity is corrected by the Bruggeman relation, $\kappa=\varepsilon^{1.5}\kappa_\infty$ where κ_∞ is the conductivity of the bulk electrolyte. Since only potential differences, and not absolute potentials, are measurable, the potential in the solution has an arbitrary datum as a boundary condition. Here, we set $\Phi_2=0$ at the positive electrode-current collector interface.

The potential in the porous electrode is determined from Ohm´s Law,

$$\nabla\Phi_1 = -\frac{i_1}{\sigma} = -\frac{\left(I-i_2\right)}{\sigma} \quad (18)$$

Where $i_1 = I - i_2$ is the current in the electrode phase and the electronic conductivity of the bulk solid is corrected for the volume fraction of the electrode by the Bruggeman relation, $\sigma=\sigma_\infty(1-\varepsilon)$, where σ_∞ is the conductivity of the nonporous composite electrode. Note that there is only one boundary condition in each electrode region. For galvanostatic operation, the boundary condition in the negative electrode is $i_2 = I$ at the negative electrode-separator interface, and in the positive electrode it is $i_2=0$ at the positive electrode-current collector interface.

Reaction Rate

The simplest type of dependence of the current density on the surface overpotential and composition adjacent to the electrode surface is given by Butler-Volmer equation:

$$i_n = i_0\left[\exp\left(\frac{\alpha_a F\left(\Phi_1-\Phi_2-U\right)}{RT}\right) - \exp\left(\frac{\alpha_c F\left(\Phi_1-\Phi_2-U\right)}{RT}\right)\right] \quad (19)$$

Here, $\eta=\Phi_1-\Phi_2-U$ is the surface overpotential, which is a driving force for an electrochemical reaction to occur. U is the open-circuit potential of the solid material evaluated at the surface concentration of the solid with respect to a hypothetical lithium reference electrode in solution just outside the diffuse part of the double layer, at the same local electrolyte concentration, and in general it is a function of solid concentration and temperature in insertion electrodes. Note that U must be specified as a function of intercalant concentration but not as a function of electrolyte concentration.

The magnitude and dependence of U on solid concentration vary considerably among different insertion materials. The shape of the open-circuit potential profile has a large effect upon the simulation results, and accurate data for this property measured with respect to a lithium reference electrode are very important, especially when one is comparing full-cell-sandwich simulations with experimental data. The anodic and cathodic transfer coefficients, α_a and α_c correspond to the fractions of the applied potential which favor the anodic and cathodic directions of the overall reaction, respectively. The exchange current density, i_0 depends on the composition of the solution adjacent to the electrode and the temperature of the electrode surface. The reaction mechanisms at electrode interfaces, particularly in the presence of the solid electrolyte interphase, are not understood in great detail. Fortunately, the rapid kinetics of electrodes used in lithium batteries reduces the importance of the exact reaction mechanism in the battery model. In the absence of more detailed information about reaction mechanisms, Butler-Volmer equation is a good approximation without comparable errors.

For the common polymer electrolyte, there is experimental evidence for a charge transfer process.

$$Li+\Theta_p \rightleftharpoons Li^+\Theta_p+e^- \quad (20)$$

Θ_p represents a site in the polymer lattice. This corresponds to an equilibrium between occupied and unoccupied lithium sites in the solid polymer electrolyte. In this case the exchange current density is defined as,

$$i_0 = F\left(k_a\right)^{\alpha_c}\left(k_c\right)^{\alpha_a}\left(c_{\max}-c\right)^{\alpha_c}\left(c\right)^{\alpha_a} \quad (21)$$

A general lithium ion insertion process is described by a charge transfer reaction,

$$Li^+ + \Theta_s + e^- \rightleftharpoons Li\Theta_s \quad (22)$$

Here, Θ_s represents a site in the solid lattice. For example, at lithium insertion in the lithium manganese oxide spinel, the corresponding reaction is given as,

$$Li^+ + Mn_2O_4 + e^- \rightleftharpoons LiMn_2O_4 \quad (23)$$

In addition, the exchange current density is given by,

$$i_0 = F\left(k_a\right)^{\alpha_c}\left(k_c\right)^{\alpha_a}\left(c_{s,\max}-c_s\right)^{\alpha_c}\left(c_s\right)^{\alpha_a}\left(c\right)^{\alpha_c} \quad (24)$$

Note that the exchange-current density tends to zero as the solid concentration approaches either 0 or $c_{s,max}$. and since the reaction-rate equation is algebraic, it requires no boundary condition.

Current Balance

The superficial current density i_2 in the pore phase is given by,

$$i_2 = F\sum_i z_i N_i \quad (25)$$

By taking the divergence of the superficial current density, we have,

$$\nabla \cdot i_2 = F \sum_i z_i \nabla \cdot N_i \quad (26)$$

By rearranging Eq. (8) and inserting it into the above equation along with considering the electroneutrality, $\sum z_i c_i = 0$, we obtain the divergence of the superficial current density in the solution.

$$\nabla \cdot i_2 = aF \sum_i z_i j_{in} = a i_n \quad (27)$$

where i_n is the average transfer current density and $\nabla \cdot i_2$ is the transfer current per unit volume of the electrode. A single electrode reaction can be written in symbolic form as,

$$\sum_k s_i M_i^{z_i} \rightarrow n e^- \quad (28)$$

where M_i is a symbol representing the chemical formula of species i and s_i is the stoichiometric coefficient of species i. From Faraday's law, the rate of electrochemical reaction is given by

$$a j_{i,n} = -\frac{a s_i}{nF} i_n = -\frac{s_i}{nF} \nabla \cdot i_2 \quad (29)$$

The specific interfacial area a is the surface area of the pore walls per unit volume of the total electrode and thus, $aj_{i,n}$ represents the rate of transfer of the species from the solid phase to the pore solution. Note that because of the electroneutrality, the divergence of the total current density is zero and can be expressed by,

$$\nabla \cdot i_1 + \nabla \cdot i_2 = 0 \quad (30)$$

By rearranging Eq. (15) and inserting into Eq. (22) in above, we can obtain the potential equation in the solution.

$$\nabla \cdot i_2 = \nabla \cdot \left(\kappa \nabla \Phi_2 \right) + \nabla \cdot \left(\kappa_D \nabla \ln c \right) = -aF j_{i,n} \quad (31a)$$

where the diffusional conductivity is given by,

$$\kappa_D = \kappa \frac{RT}{F} \left(1 - t_+^0 \right) \cdot \left(1 + \frac{d \ln f_A}{d \ln c} \right) \quad (31b)$$

Considering Eq. (18) and by applying equation (30), the potential equation in the electrode can be expressed as,

$$\nabla \cdot i_1 = \nabla \cdot \left(\sigma \nabla \Phi_1 \right) = -\nabla \cdot i_2 = aF j_{i,n} \quad (32)$$

Energy Balance

A single cell in most LIB packs used in industry currently is very thin, less than 300μm, so the temperature gradients perpendicular to the electrodes are negligible, considering only the Joule and Peltier heating. Therefore, the heat generation in a 1D model assumes uniform temperature in an individual cell. Once the heat generation in each cell is calculated, it can be inserted into a standard heat transfer equation for the battery geometry, to calculate temperature changes across a tall cell or battery stack. Such models are generally concerned with temperature gradients in two- or three-dimensions. The calculation of the heat generated by a cell and the temperature changes in a cell stack requires an energy balance in a cell. Here, we revisit the energy balance equations

in Rao and Newman [16], which presents a form of Bernardi et al.´s energy balance. Considering a single cell and from the first law of thermodynamics,

$$\frac{dH_{tot}}{dt} = \dot{Q} - IV \quad (33)$$

where H_{tot} is the sum of the enthalpy of the species, Q the rate of heat transfer with the surrounding, and IV is the electrical work. The average form of total enthalpy over a small volume element of the cell is given by,

$$\frac{dH_{tot}}{dt} = \frac{d}{dt}\int_v \sum_j \sum_i \varepsilon_j \langle c_{i,j} \rangle \bar{H}_{i,j}^{ref} \quad (34)$$

Here, $\langle c_{i,j} \rangle$ is the concentration of species i averaged locally over phase j, in the way that $\varepsilon \langle c_{i,j} \rangle$ is a superficial concentration. $\bar{H}_{i,j}^{ref}$ refers to the average enthalpy at a reference concentration. Differentiation of the product in the integral in the above equation:

$$\frac{dH_{tot}}{dt} = \int_v \sum_j \sum_i \left[\frac{\partial \varepsilon_j \langle c_{i,j} \rangle}{\partial t} \bar{H}_{i,j}^{ref} + \varepsilon_j \langle c_{i,j} \rangle \frac{\partial \bar{H}_{i,j}^{ref}}{\partial T} \cdot \frac{\partial T}{\partial t} \right] dv \quad (35)$$

Here, it can be identified the heat capacity of the system as,

$$C_p = \int_v \sum_j \sum_i \varepsilon_j \langle c_{i,j} \rangle \bar{C}_{pi,j}^{ref} dv \quad (36)$$

and ignoring the heat of mixing by flux term, but considering only the rate of transfer of the species, $aj_{i,n}$,

$$\frac{dH_{tot}}{dt} = C_p \cdot \frac{dT}{dt} + \int_v \sum_j \sum_i aj_{i,n} \bar{H}_{i,j}^{ref} dv \quad (37)$$

Considering Faraday's law,

$$aj_{i,n} = -\sum_l \frac{s_{i,l}}{n_l F} ai_{n,l} \quad (38)$$

Then, Eq. (37) becomes,

$$\frac{dH_{tot}}{dt} = C_p \cdot \frac{dT}{dt} - \sum_l \int_v \sum_j \sum_i \frac{s_{i,l}}{n_l F} ai_{n,l} \bar{H}_{i,j}^{ref} dv \quad (39)$$

By introducing the reaction enthalpy change or the enthalpy potential,

$$\Delta H_l = U_{H,l} = -\sum_j \sum_i \frac{s_{i,l}}{n_l F} \bar{H}_{i,j}^{ref} = -T^2 \frac{d}{dT}\left(\frac{U_l}{T}\right) = U_l - T\frac{dU_l}{dT} \quad (40)$$

where U_l is the open circuit potential of reaction l.

By substituting Eq. (40) into Eq. (39), the total enthalpy change becomes,

$$\frac{dH_{tot}}{dt} = C_p \cdot \frac{dT}{dt} + \int_v \sum_l ai_{n,l} U_{H,l} dv$$
$$= C_p \cdot \frac{dT}{dt} + \int_v \sum_l ai_{n,l} \left(U_l - T \frac{dU_l}{dT} \right) dv \quad (41)$$

Finally, if we insert Eq. (41) into Eq. (33), we can have the energy balance relating the heat generation.

$$C_p \cdot \frac{dT}{dt} - \dot{Q} = -\int_v \sum_l ai_{n,l} \left(U_l - T \frac{dU_l}{dT} \right) dv - IV \quad (42)$$

Note that we ignored here the concentration dependence of the heating, which is in general small compared to the other heating mechanisms.

Alternatively, in contrast to the thermodynamic approach, the energy balance can be derived by a local heat generation method. Let the left interface between the anode and current collector lie at x=0, and extend to $x=x_1$, the separator extend from $x=x_1$ to $x=x_2$, and the composite cathode from $x=x_2$ to $x=x_3$. The heat generation at an interface consists of two contributions: reversible and irreversible.

$$-\dot{q} = i\left(\Pi + \eta\right) \quad (43)$$

where Π is Peltier coefficient and η is the overpotential between the electrode and electrolyte. Detailed derivation of the interface heat generation can be found in Appendix B[15]. The reversible heat, $i\Pi$ is the sum of the corresponding anode and cathode for a whole reaction. So, if the temperature is the same for the anode and the cathode, this reversible heat generation rate is reduced to the usual thermodynamic heat effect, i.e. the entropy change rate for the cell, TdS/dt.

The irreversible heat generation rate due to electrochemical reaction at the composite anode and cathode are,

$$-\overline{q}_a^{\eta} = \int_{x_0}^{x_1} ai_n \eta_a dx \quad (44a)$$

$$-\overline{q}_c^{\eta} = \int_{x_2}^{x_3} ai_n \eta_c dx \quad (44b)$$

The Joule heating rate due to ohmic losses in solid and electrolyte is $-i \cdot \nabla\Phi$. Let the subscript 1 be for the solid and 2 for the electrolyte. The heat generation in an electrolyte is rather complicated when there is a concentration gradient. However, we ignore the thermal effect of any concentration gradient in the electrolyte again. So, the heat generation in the separator is directly linked to the potential difference in the electrolyte between the two faces of the separator.

$$-\dot{q}_s^J = i\Delta\Phi_s, \ \Delta\Phi_s = \Phi_2\left(x_1\right) - \Phi_2\left(x_2\right) \quad (45)$$

In the porous electrodes, the heat generation rate in the electrolyte and active matrix are,

$$-\dot{q}_a^J = \int_{x_0}^{x_1} \left(-i_1 \frac{d\Phi_1}{dx} - i_2 \frac{d\Phi_2}{dx} \right) dx \quad (46a)$$

$$-\dot{q}_c^J = \int_{x_2}^{x_3} \left(-i_1 \frac{d\Phi_1}{dx} - i_2 \frac{d\Phi_2}{dx} \right) dx \quad (46b)$$

Therefore, total irreversible heat generation is given by combining all equations.

$$-\dot{q} = i\Delta\Phi_s + \int_{x_0}^{x_1}\left(ai_n\eta_a - i_1\frac{d\Phi_1}{dx} - i_2\frac{d\Phi_2}{dx}\right)dx + \int_{x_2}^{x_3}\left(ai_n\eta_c - i_1\frac{d\Phi_1}{dx} - i_2\frac{d\Phi_2}{dx}\right)dx \quad (47)$$

Now, by applying integration by parts,

$$-\dot{q} = i\left[\Phi_2(x_1) - \Phi_2(x_1)\right] + i\Phi_1\big|_{x_0} - i\Phi_2\big|_{x_1} - i\Phi_1\big|_{x_3} + i\Phi_2\big|_{x_2} + \int_{x_0}^{x_1}\left(ai_n\eta_a + \frac{di_1}{dx}\cdot\Phi_1 + \frac{di_2}{dx}\cdot\Phi_2\right)dx + + \int_{x_2}^{x_3}\left(ai_n\eta_c + \frac{di_1}{dx}\cdot\Phi_1 + \frac{di_2}{dx}\cdot\Phi_2\right)dx \quad (48)$$

Here, we used the current boundary conditions for each interface. For example, $i_1=i$ and $i_2=0$ at $x=x_0$. It is assumed that the reference potential at $x=x_0$ is equal to zero, $\Phi_1(x_0)=0$ and thus, the cell potential is $V=\Phi_1(x_3)$. In addition, consider the relation between the normal flux and the divergence of the current as,

$$ai_n = \frac{di_2}{dx} = -\frac{di_1}{dx} \quad (49)$$

Then, the total heat generation becomes,

$$-\dot{q} = \int_{x_0}^{x_1} ai_n\left(\eta_a - \Phi_1 + \Phi_2\right)dx + \int_{x_2}^{x_3} ai_n\left(\eta_c - \Phi_1 + \Phi_2\right)dx - iV \quad (50)$$

Since,

$$\eta_a = \Phi_1 - \Phi_2 - U_a \text{ ,and } \eta_c = \Phi_1 - \Phi_2 - U_c$$

and adding the reversible term into the integral, the final form of the heat generation can be expressed as,

$$-\dot{q} = \int_{x_0}^{x_1} ai_n\left(U_a - T\frac{dU_a}{dT}\right)dx + \int_{x_2}^{x_3} ai_n\left(U_c - T\frac{dU_c}{dT}\right)dx - iV \quad (51)$$

Note that the above equation is the same as Eq.(42) if we add inside terms of integration except the unsteady term.

For the scaled-up battery geometry, one can use a standard heat transfer equation to calculate temperature changes across a cell stack or battery pack.

$$\frac{\partial}{\partial t}\left(\rho c_p T\right) + \nabla\cdot\left(\mathbf{v}T\right) = \nabla\cdot\left(\lambda\nabla T\right) + \dot{q} \quad (52)$$

LIB Models

In the previous sections, we described or derived all equations needed for LIB models. It is noted that the mass transports equations are partial differential equations, both the potential equations and the current equation are ordinary differential equations, and the reaction rate, the Butler-Volmer model is an algebraic equation. In case of not needing to explicitly calculate j_{in} and i_2, the two equations may be combined into one equation.

i) 6 equation model: The first full electrochemical model which was first presented by Doyle, Fuller, and Newman [8,9] can be completed using Eq. (12), (15), (17), (18), (19), and (29) for the 6 unknown variables: c, c_s, Φ_1, Φ_2, i_2, and j.

To describe the electrochemical performance of the cell, the coupled governing equations must be solved simultaneously. It is important to note that since the Butler-Volmer equation makes the system nonlinear, the equation involving it as a source term must be linearized to ensure the convergence.

ii) 4 equation model: Equation (12), (15), (31), and (32) can constitute a complete set of model equations for the first 4 unknown variables in the previous model. After solving all equations either coupled or sequentially, the superficial current density is determined in terms of either potential gradient in the electrode (or electrolyte) phase or the interfacial transfer current density. However, Eq.(31) and (32) must be carefully solved since the source term, Butler-Volmer equation, is strongly nonlinear, indicating that it should be well treated with linearization process before solving the implicit iteration for them.

Results and Discussion

The open circuit potential which sometimes called the equilibrium potential is in general given as a function of the amount of lithium inserted (solid concentration) and and temperature by an experimental data. Fig.1(a) and (b) show the open circuit potential for the graphite, LiC_6 of the anode and $LiMn_2O_4$ of the cathode.

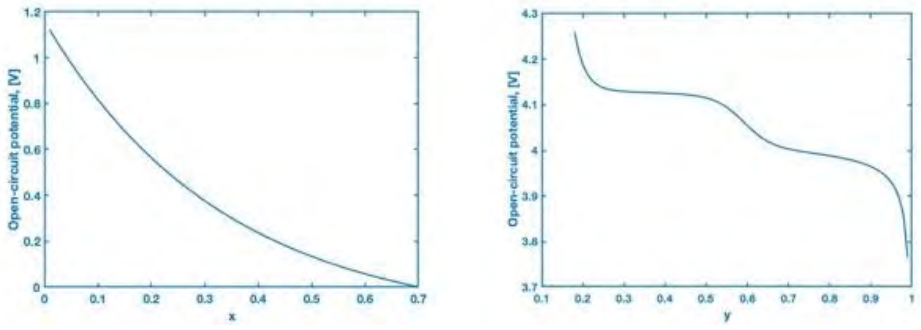

(a) (b)

Figure 1 Open circuit potential curves: (a) LiC_6 of the anode, and (b) $LiMn_2O_4$ of the cathode.

Figure 2(a) shows the problem descriptions of the rigid ball impacting on the cell stack which consists of 10 cells of LIBs. Each cell has the negative current collector(10 μm), anode composite electrode(100 μm), separator(52 μm), cathode composite electrode(174 μm), and positive current collector(10 μm), respectively. Since the cell stack accumulates serially, the total thickness of the cell stack measures 3.46 mm. To protect the LIB stack, the steel case of 1mm covers the outside of the battery. Thus, overall dimension of the LIB model in present study has 317 mm x 97 mm x 5.46 mm as shown in Fig. 2(a). It should be noted that each solver in LS-DYNA can be assigned an independent part to solver in its own region. For example, the electrochemical battery solver can be assigned to solve only part 1~3, which covered all battery parts, while the thermal solver solves all parts except the rigid ball which assigned to the mechanical solver that includes the other parts. In addition, each electrochemical cell has 220 mesh points in the current flowing direction, x-direction. Therefore, one can consider it as a simple battery-thermal-mechanical interacting(BTMI) problem since the battery solver has its own 1D mesh system in each battery structural elements, and also, the thermal-mechanical solver has its own 3D mesh system.

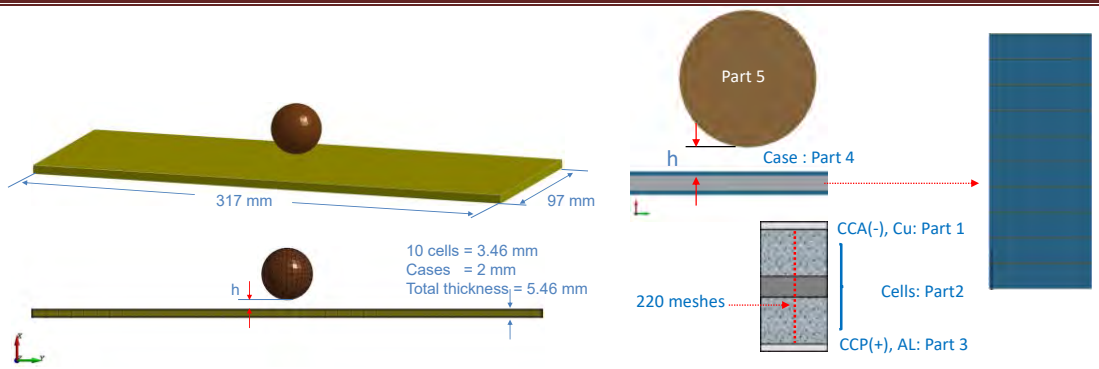

(a) (b)

Figure 2 Schematics of the ball impact on the 10 cells of LIB and detailed set up of the problem with corresponding to parts.

Figure 3(b) shows validation curves compared with well known simulation and experiment data [17] for the discharge capacity as a function of time calculated at different current densities from 1.75 A/m^2 to 35 A/m^2. Doyle and Newman [17] calculated both with/without film resistance in each case and they compared with experiment data showing good agreement. In the present study, we only compared with no film resistance case showing good agreement with their curves.

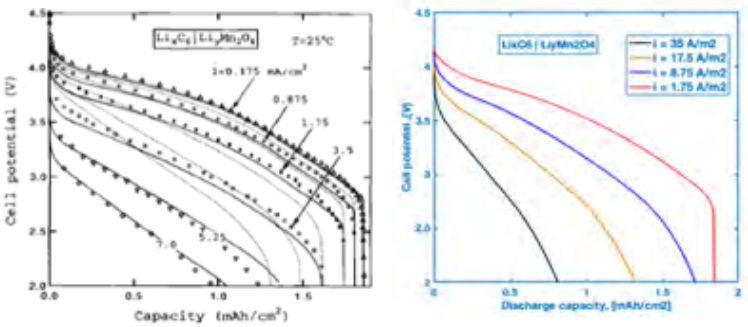

(a) John Newman (b) LS-DYNA model

Figure 3 Validation of discharge capacity of the LMO based LIB model.

The coupling from the electrochemical solver to the thermal and mechanical solver is not easy process. It is mostly due to the different time scales among the solvers. Since the electric current flow is assumed to be in a steady-state, and the reaction on the boundary between the solid electrode and the electrolyte is extremely fast, therefore, in general, the time step in the battery solver is of the order of a second. By contrast, the mechanical time step is based on the Courant number, which is proportion to the time step divided by the speed of sound in the media, and is of the order of the nanosecond to microsecond. To resolve the disparity of the time scales, we use a strategy of employing different schemes in the mechanical solver. For example, before the rigid ball impact on the battery stack, the implicit scheme of the mechanical solver was activated and after the rigid ball contacts the cell stack, the mechanical solver is switched to the explicit scheme. It is noted that while running the implicit scheme, the battery and thermal solver were activated with a strong numerical coupling to each other. In this way, we can simulate and complete the three way couplings among the solvers. The mechanical properties of the LIB such as Yong's modulus and Poisson's ratio was averaged with weighting factor based on length scale of each layer [17]. Figure 4 shows the snapshot at times right after the rigid ball initially

contacts the LIB cell stack. As can clearly be seen, a hot spot develops at 6 second after the ball contacts the LIB cell stack, meaning that the temperature inside of LIB starts to increase.

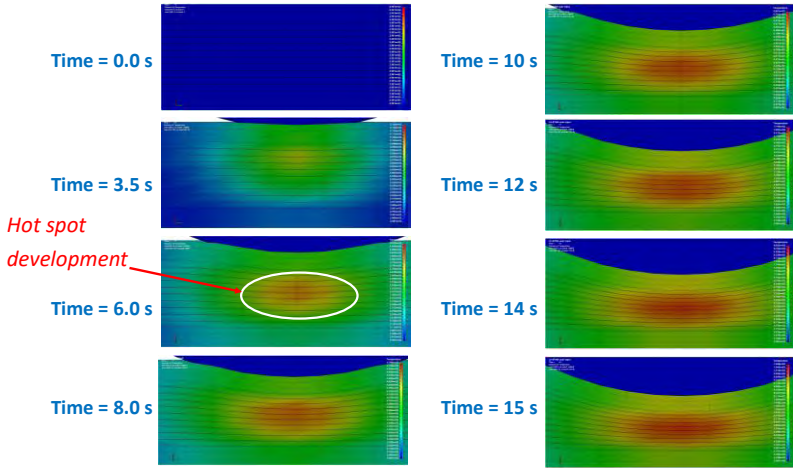

Figure 4 Time evolution snap shot after the ball impacted 10 cells of LIB stack.

In case of a cell temperature increasing to a critical thresholding temperature like the melting point of the lithium, 453K at which stage the thermal runaway starts, and eventually a fire or explosion takes place, there is no way to control or suppress such a temperature increase as shown in Fig. 5(a) and (c).

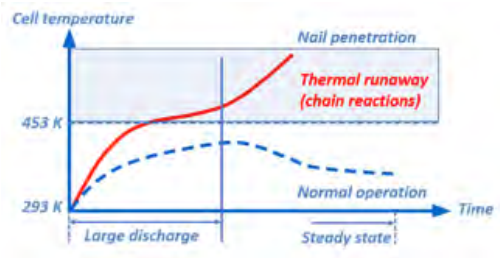

$$DT(x,t) = \frac{1}{H}\int_0^t q'''_{total}\,dt', \quad q'''_{total} = (Joule + Peltier)\ heating$$

(a)

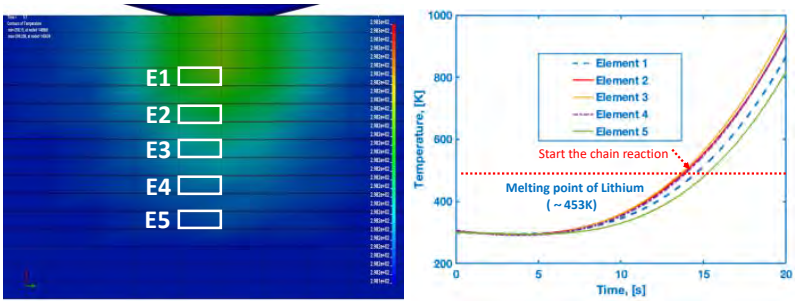

(b) (c)

Figure 5 Analysis of the thermal runaways: (a) conceptional estimation of thermal runaway based on joule and Peltier heating modes, (b) individual cell elements inside battery cell stack, and (c) corresponding temperature increasing as function of time at each element.

During the deformation by impacting force, a cell's temperature increases due to both Joule heating and Peltier heating, which is mostly due to an exothermal reaction initiated by the entropy changes inside of the battery cell. Figure 5(b) shows the individual cell elements inside LIB stack to monitor the temperature changes as function of time and Figure 5(c) shows the temperature increasing of each cell elements. As positioned in Figure 4, the rapid increasing of the temperature starts about 6s after the ball was in contact. After that point, temperatures in all elements increases exponentially to the thermal runaway. Although the present study is not modelling any chemical reaction mechanism, it is speculated that the chain reactions could be started after reaching the melting point of the lithium metal at 453 K.

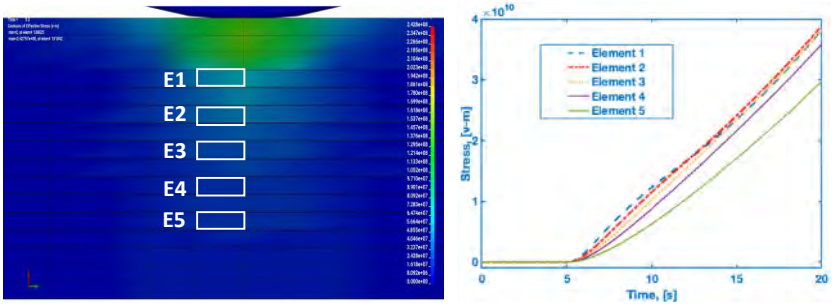

(a) (b)

Figure 6 Stress analysis inside battery stack induced by impacting ball: (a) individual cell elements inside cell stack, and (b) corresponding Von Mises stress responses as a function of time at each element.

Figure 6 (a) and (b) show the individual elements of interesting and the corresponding changes of their Von Mises stress. Similarly, although much of stress is loaded on the steel case of LIB(not shown in Figure 6), the phenomena of battery cell stress increasing has the same trends as the temperature increasing in Fig. 5. More detailed studies on the relation between stress and temperature could be a topic for the future research, and is beyond the scope of the present study.

Summary

In this presentation, we report a new development of the electrochemical-thermal-mechanical coupling based on previously developed electrochemical LIB model in LS-DYNA®. In 10 cells of a lithium ion battery stack, each cell consists of Graphite(LiC_6) anode/Separator/high performance layered LMO($LiMn_2O_4$) cathode, which has been strongly proposed as a candidate for automotive batteries because of its high capacity, thermal stability, and low volume change rate (cycle performance). For the thermal-mechanical analysis, each layer in a cell and outside cases are modeled corresponding to their material properties. Then, a rigid ball impacts the center top position of the cell stack in order to investigate the thermal and mechanical responses of a lithium ion battery stack. To see the cell responses inside LIB, we selected the first 20 seconds of the time period during the initial discharging process of the battery operation. The results show that a hot spot was developed in a few seconds of deformation and the rapid temperature increase over the melting point of the lithium was detected, where the thermal runaway eventually takes place. In addition, with the present development of the battery-thermal-mechanical interaction, we strongly believe that users can apply this to more complex applications such as a cellular phone deformation and even EV battery deformation test in automotive industries.

References

[1] D. Linden and T. B. Reddy. Handbook of Batteries. McGraw-Hill Companies, Inc., New York, 3rd edition, 2002.

[2] C. Mikolajczak, M. Kahn, K. White, and R. T. Long. Lithium-Ion Batteries Hazard and Use Assessment. Technical Report July, Exponent Failure Analysis Associates, Inc., 2011.

[3] Y. Xia, T. Wierzbicki, E. Sahraei, X. Zhang, J. Power Sources 267 78-97, 2014.

[4] Y. Chen and J. W. Evans, J. Electrochem. Soc., 140, 1833, 1993.

[5] Y. Chen and J. W. Evans, J. Electrochem. Soc., 141, 2947, 1994.

[6] C. R. Pal and J. Newman, J. Electrochem. Soc., 142, 3282, 1995.

[7] Li Song and J. W. Evans, J. Electrochem. Soc., 147, 2086, 2000.

[8] M. Doyle, T.F. Fuller, and J. Newman, *J. Electrochem. Soc*., 140, 1526, 1993.

[9] T.F. Fuller, M. Doyle, and J. Newman, *J. Electrochem. Soc*., 141, 1, 1994.

[10] E. J. Cheng, N. J. Taylor, J. Wolfenstine, J. Sakamoto, *J. Asian Ceramic Societies*, 5, 113, 2017.

[11] J. Newman and W. Tiedmann, *AIChE J*., 21. 25, 1975

[12] R. B. Bird, W.E. Stewart, and E.N. Lightfoot, "*Transport Phenomena*" John Wiley and Sons, Inc. New York, 1960.

[13] L. Onsager, *Annals New York Acad. Science*, 46, 242,1945.

[14] J. Newman and Karen E. Thomas-Alyea, "*Electrochemical Systems*", 3rd Edition, John Wiley and Sons, Inc. New Jersey, (2004).

[15] 2020 LS-DYNA Multi-Physics Theory Manual at www.lstc.com.

[16] L. Rao and J. Newman, *J. Electrochem. Soc*., 144, 2697, 1997.

[17] M. Doyle, J. Newman, A. S. Gozdz, C. N. Schmutz, and J.-M. Tarascon, *J. Electrochem. Soc*., Vol 143, No 6 1890, 1996.

BETA CAE Systems. www.beta-cae.com

BETA CAE Systems - ANSA

An advanced multidisciplinary CAE pre-processing tool that provides all the necessary functionality for full-model build up, from CAD data to ready-to-run solver input file, in a single integrated environment. ANSA is a full product modeler for LS-DYNA, with integrated Data Management and Process Automation. ANSA can also be directly coupled with LS-OPT of LST, an ANSYS company to provide an integrated solution in the field of optimization.

BETA CAE Systems μETA

Is a multi-purpose post-processor meeting diverging needs from various CAE disciplines. It owes its success to its impressive performance, innovative features and capabilities of interaction between animations, plots, videos, reports and other objects. It offers extensive support and handling of LS-DYNA 2D and 3D results, including those compressed with SCAI's FEMZIP software.

Solutions for:

Process Automation - Data Management – Meshing – Durability - Crash & Safety NVH - CFD - Thermal analysis - Optimization - Powertrain
Products made of composite materials - Analysis Tools -
Maritime and Offshore Design - Aerospace engineering - Biomechanics

ETA – Engineering Technology Associates www.eta.com
etainfo@eta.com

Inventium Suite™

Inventium Suite™ is an enterprise-level CAE software solution, enabling concept to product. Inventium's first set of tools will be released soon, in the form of an advanced Pre & Post processor, called PreSys.

Inventium's unified and streamlined product architecture will provide users access to all of the suite's software tools. By design, its products will offer a high performance modeling and post-processing system, while providing a robust path for the integration of new tools and third party applications.

PreSys

Inventium's core FE modeling toolset. It is the successor to ETA's VPG/PrePost and FEMB products. PreSys offers an easy to use interface, with drop-down menus and toolbars, increased graphics speed and detailed graphics capabilities. These types of capabilities are combined with powerful, robust and accurate modeling functions.

VPG

Advanced systems analysis package. VPG delivers a unique set of tools which allow engineers to create and visualize, through its modules--structure, safety, drop test, and blast analyses.

DYNAFORM

Complete Die System Simulation Solution. The most accurate die analysis solution available today. Its formability simulation creates a "virtual tryout", predicting forming problems such as cracking, wrinkling, thinning and spring-back before any physical tooling is produced.

ESI Group www.esi-group.com

Visual-Environment is an integrative simulation platform for simulation tools operating either concurrently or standalone for various solver. Comprehensive and integrated solutions for meshing, pre/post processing, process automation and simulation data management are available within same environment enabling seamless execution and automation of tedious workflows. This very open and versatile environment simplifies the work of CAE engineers across the enterprise by facilitating collaboration and data sharing leading to increase of productivity.

Visual-Crash DYNA provides advanced preprocessing functionality for LS-DYNA users, e.g. fast iteration and rapid model revision processes, from data input to visualization for crashworthiness simulation and design. It ensures quick model browsing, advanced mesh editing capabilities and rapid graphical assembly of system models. Visual-Crash DYNA allows graphical creation, modification and deletion of LS-DYNA entities. It comprises tools for checking model quality and simulation parameters prior to launching calculations with the solver. These tools help in correcting errors and fine-tuning the model and simulation before submitting it to the solver, thus saving time and resources.
Several high productivity tools such as advanced dummy positioning, seat morphing, belt fitting and airbag folder are provided in **Visual-Safe,** a dedicated application to safety utilities.

Visual-Mesh is a complete meshing tool supporting CAD import, 1D/2D/3D meshing and editing for linear and quadratic meshes. It supports all meshing capabilities, like shell and solid automesh, batch meshing, topo mesh, layer mesh, etc. A convenient Meshing Process guides you to mesh the given CAD component or full vehicle automatically.

Visual-Viewer built on a multi-page/multi-plot environment, enables data grouping into pages and plots. The application allows creation of any number of pages with up to 16 windows on a single page. These windows can be plot, animation, video, model or drawing block windows. Visual-Viewer performs automated tasks and generates customized reports and thereby increasing engineers' productivity.

Visual-Process provides a whole suite of generic templates based on LS-DYNA solver (et altera). It enables seamless and interactive process automation through customizable LS-DYNA based templates for automated CAE workflows.

All generic process templates are easily accessible within the unique framework of Visual-Environment and can be customized upon request and based on customer's needs.

Visual*DSS* is a framework for Simulation Data and Process Management which connects with Visual-Environment and supports product engineering teams, irrespective of their geographic location, to make correct and realistic decisions throughout the virtual prototyping phase. Visual*DSS* supports seamless connection with various CAD/PLM systems to extract the data required for building virtual tests as well as building and chaining several virtual tests upstream and downstream to achieve an integrated process. It enables the capture, storage and reuse of enterprise knowledge and best practices, as well as the automation of repetitive and cumbersome tasks in a virtual prototyping process, the propagation of engineering changes or design changes from one domain to another.

JSOL Corporation www.jsol.co.jp/english/cae/

HYCRASH

Easy-to-use one step solver, for Stamping-Crash Coupled Analysis. HYCRASH only requires the panels' geometry to calculate manufacturing process effect, geometry of die are not necessary. Additionally, as this is target to usage of crash/strength analysis, even forming analysis data is not needed. If only crash/strength analysis data exists and panel ids is defined. HYCRASH extract panels to calculate it's strain, thickness, and map them to the original data.

JSTAMP/NV

As an integrated press forming simulation system for virtual tool shop the JSTAMP/NV meets the various industrial needs from the areas of automobile, electronics, iron and steel, etc. The JSTAMP/NV gives satisfaction to engineers, reliability to products, and robustness to tool shop via the advanced technology of the JSOL Corporation.

JMAG

JMAG uses the latest techniques to accurately model complex geometries, material properties, and thermal and structural phenomena associated with electromagnetic fields. With its excellent analysis capabilities, JMAG assists your manufacturing process.

LST

Livermore Software Technology, an ANSYS Company
www.lstc.com

LS-DYNA

A general-purpose finite element program capable of simulating complex real world problems. It is used by the automobile, aerospace, construction, military, manufacturing, and bioengineering industries. LS-DYNA is optimized for shared and distributed memory Unix, Linux, and Windows based, platforms, and it is fully QA'd by LST, an ANSYS company. The code's origins lie in highly nonlinear, transient dynamic finite element analysis using explicit time integration.

LS-PrePost

An advanced pre and post-processor that is delivered free with LS-DYNA. The user interface is designed to be both efficient and intuitive. LS-PrePost runs on Windows, Linux, and Macs utilizing OpenGL graphics to achieve fast rendering and XY plotting.

LS-OPT

LS-OPT is a standalone Design Optimization and Probabilistic Analysis package with an interface to LS-DYNA. The graphical preprocessor LS-OPTui facilitates definition of the design input and the creation of a command file while the postprocessor provides output such as approximation accuracy, optimization convergence, tradeoff curves, anthill plots and the relative importance of design variables.

LS-TaSC

A Topology and Shape Computation tool. Developed for engineering analysts who need to optimize structures, LS-TaSC works with both the implicit and explicit solvers of LS-DYNA. LS-TaSC handles topology optimization of large non-linear problems, involving dynamic loads and contact conditions.

LST, AN ANSYS COMPANY Dummy Models

Anthropomorphic Test Devices (ATDs), as known as "crash test dummies", are life-size mannequins equipped with sensors that measure forces, moments, displacements, and accelerations.

LST, AN ANSYS COMPANY Barrier Models

LSTC offers several Offset Deformable Barrier (ODB) and Movable Deformable Barrier (MDB) model.

Material Sciences Corporation www.materials-sciences.com

Materials Sciences Corporation has provided engineering services to the composites industry since 1970. During this time, we have participated in numerous programs that demonstrate our ability to: perform advanced composite design, analysis and testing; provide overall program management; work in a team environment; and transition new product development to the military and commercial sectors. MSC's corporate mission has expanded beyond basic research and development now to include transitioning its proprietary technologies from the research lab into innovative new products. This commitment is demonstrated through increased staffing and a more than 3-fold expansion of facilities to allow in-house manufacturing and testing of advanced composite materials and structures.

Materials Sciences Corporation (MSC) MAT161/162 - enhanced features have been added to the Dynamic Composite Simulator module of LS-DYNA.

This enhancement to LS-DYNA, known as MAT161/162, enables the most effective and accurate dynamic progressive failure modeling of composite structures to enable the most effective and accurate dynamic progressive failure modeling of composite structures currently available.

MSC/LS-DYNA Composite Software and Database -

Fact Sheet: http://www.materials-sciences.com/dyna-factsheet.pdf

- MSC and LSTC have joined forces in developing this powerful composite dynamic analysis code.
- For the first time, users will have the enhanced ability to simulate explicit dynamic engineering problems for composite structures.
- The integration of this module, known as 'MAT 161', into LS-DYNA allows users to account for progressive damage of various fiber, matrix and interply delamination failure modes.
- Implementing this code will result in the ability to optimize the design of composite structures, with significantly improved survivability under various blast and ballistic threats.

MSC's LS-DYNA module can be used to characterize a variety of composite structures in numerous applications—such as this composite hull under blast.

Oasys Ltd. LS-DYNA Environment www.oasys-software.com/dyna

The Oasys Suite of software is exclusively written for LS-DYNA® and is used worldwide by many of the largest LS-DYNA® customers. The suite comprises of:

Oasys PRIMER

Key benefits:

- Pre-Processor created specifically for LS-DYNA®
- Compatible with the latest version of LS-DYNA®
- Maintains the integrity of data
- Over 6000 checks and warnings – many auto-fixable
- Specialist tools for occupant positioning, seatbelt fitting and seat squashing (including setting up pre-simulations)
- Many features for model modification, such as part replace
- Ability to position and depenetrate impactors at multiple locations and produce many input decks automatically (e.g. pedestrian impact, interior head impact)
- Contact penetration checking and fixing
- Connection feature for creation and management of connection entities.
- Support for Volume III keywords and large format/long labels
- Powerful scripting capabilities allowing the user to create custom features and processes

www.oasys-software.com/dyna

Oasys D3PLOT

Key benefits:

- Powerful 3D visualization post-processor created specifically for LS-DYNA®
- Fast, high quality graphics
- Easy, in-depth access to LS-DYNA® results
- Scripting capabilities allowing the user to speed up post-processing, as well as creating user defined data components

www.predictiveengineering.com

Predictive Engineering provides finite element analysis consulting services, software, training and support to a broad range of engineering companies across North America. We strive to exceed client expectations for accuracy, timeliness and knowledge transfer. Our process is both cost-effective and collaborative, ensuring all clients are reference clients.

Our mission is to be honest brokers of information in our consulting services and the software we represent.

Our History

Since 1995, Predictive Engineering has continually expanded its client base. Our clients include many large organizations and industry leaders such as SpaceX, Nike, General Electric, Navistar, FLIR Systems, Sierra Nevada Corp, Georgia-Pacific, Intel, Messier-Dowty and more. Over the years, Predictive Engineering has successfully completed more than 800 projects, and has set itself apart on its strong FEA, CFD and LS-DYNA consulting services.

恒士达科技
Hengstar Tech.

Shanghai Hengstar www.hengstar.com

Center of Excellence: Hengstar Technology is the first LS-DYNA training center of excellence in China. As part of its expanding commitment to helping CAE engineers in China, Hengstar Technology will continue to organize high level training courses, seminars, workshops, forums etc., and will also continue to support CAE events such as: China CAE Annual Conference; China Conference of Automotive Safety Technology; International Forum of Automotive Traffic Safety in China; LS-DYNA China users conference etc.

On Site Training: Hengstar Technology also provides customer customized training programs on-site at the company facility. Training is tailored for customer needs using LS-DYNA such as material test and input keyword preparing; CAE process automation with customized script program; Simulation result correlation with the test result; Special topics with new LS-DYNA features etc..

Distribution & Support: Hengstar distributes and supports LS-DYNA, LS-OPT, LS-Prepost, LS-TaSC, LSTC FEA Models; Hongsheng Lu, previously was directly employed by LSTC before opening his distributorship in China for LSTC software. Hongsheng visits LSTC often to keep update on the latest software features.

Hengstar also distributes and supports d3View; Genesis, Visual DOC, ELSDYNA; Visual-Crash Dyna, Visual-Process, Visual-Environment; EnkiBonnet; and DynaX & MadyX etc.

Consulting

As a consulting company, Hengstar focuses on LS-DYNA applications such as crash and safety, durability, bird strike, stamping, forging, concrete structures, drop analysis, blast response, penetration etc with using LS-DYNA's advanced methods: FEA, ALE, SPH, EFG, DEM, ICFD, EM, CSEC..

Cloud - HPC Services - Subscription JSOL

Contact: JSOL Corporation Engineering Technology Division cae-info@sci.jsol.co.jp

Cloud computing services
for
JSOL Corporation LS-DYNA users in Japan

JSOL Corporation is cooperating with chosen cloud computing services

JSOL Corporation, a Japanese LS-DYNA distributor for Japanese LS-DYNA customers.

LS-DYNA customers in industries / academia / consultancies are facing increased needs for additional LS-DYNA cores

In calculations of optimization, robustness, statistical analysis, we find that an increase in cores of LS-DYNA are needed, for short term extra projects or cores.

JSOL Corporation is cooperating with some cloud computing services for JSOL's LS-DYNA users and willing to provide short term license.

This service is offered to customers using Cloud License fee schedule, the additional fee is less expensive than purchasing yearly license.

The following services are available (only in Japanese). HPC OnLine:

NEC Solution Innovators, Ltd. - http://jpn.nec.com/manufacture/machinery/hpc_online/

Focus - Foundation for Computational Science
http://www.j-focus.or.jp

Platform Computation Cloud - CreDist.Inc.

PLEXUS CAE
Information Services International-Dentsu, Ltd. (ISID) https://portal.plexusplm.com/plexus-cae/

SCSK Corporation - http://www.scsk.jp/product/keyword/keyword07.html

Cloud - HPC Services - Subscription RESCALE

www.rescale.com

Rescale: Cloud Simulation Platform

The Power of Simulation Innovation

We believe in the power of innovation. Engineering and science designs and ideas are limitless. So why should your hardware and software be limited? You shouldn't have to choose between expanding your simulations or saving time and budget.

Using the power of cloud technology combined with LS-DYNA allows you to:

- Accelerate complex simulations and fully explore the design space
- Optimize the analysis process with hourly software and hardware resources
- Leverage agile IT resources to provide flexibility and scalability

True On-Demand, Global Infrastructure

Teams are no longer in one location, country, or even continent. However, company data centers are often in one place, and everyone must connect in, regardless of office. For engineers across different regions, this can cause connection issues, wasted time, and product delays.

Rescale has strategic/technology partnerships with infrastructure and software providers to offer the following:

- Largest global hardware footprint – GPUs, Xeon Phi, InfiniBand
- Customizable configurations to meet every simulation demand
- Worldwide resource access provides industry-leading tools to every team
- Pay-per-use business model means you only pay for the resources you use
- True on-demand resources – no more queues

ScaleX Enterprise: Transform IT, Empower Engineers, Unleash Innovation

The ScaleX Enterprise simulation platform provides scalability and flexibility to companies while offering enterprise IT and management teams the opportunity to expand and empower their organizations.

Rescale Cloud Simulation Platform

www.rescale.com

ScaleX Enterprise allows enterprise companies to stay at the leading edge of computing technology while maximizing product design and accelerating the time to market by providing:

- Collaboration tools
- Administrative control
- API/Scheduler integration
- On-premise HPC integration

Industry-Leading Security

Rescale has built proprietary, industry-leading security solutions into the platform, meeting the needs of customers in the most demanding and competitive industries and markets.

- Manage engineering teams with user authentication and administrative controls
- Data is secure every step of the way with end-to-end data encryption
- Jobs run on isolated, kernel-encrypted, private clusters
- Data centers include biometric entry authentication
- Platforms routinely submit to independent external security audits

Rescale maintains key relationships to provide LS-DYNA on demand on a global scale. If you have a need to accelerate the simulation process and be an innovative leader, contact Rescale or the following partners to begin running LS-DYNA on Rescale's industry-leading cloud simulation platform.

LSTC - DYNAmore GmbH JSOL Corporation

Rescale, Inc. - 1-855-737-2253 (1-855-RESCALE) - info@rescale.com

944 Market St. #300, San Francisco, CA 94102 USA

ESI Cloud Based Virtual Engineering Solutions

www.esi-group.com

ESI Cloud offers designers and engineers cloud-based computer aided engineering (CAE) solutions across physics and engineering disciplines.

ESI Cloud combines ESI's industry tested virtual engineering solutions integrated onto ESI's Cloud Platform with browser based modeling,

With ESI Cloud users can choose from two basic usage models:

- An end-to-end SaaS model: Where modeling, multi-physics solving, results visualization and collaboration are conducted in the cloud through a web browser.
- A Hybrid model: Where modeling is done on desktop with solve, visualization and collaboration done in the cloud through a web browser.

Virtual Performance Solution:

ESI Cloud offers ESI's flagship Virtual Performance Solution (VPS) for multi-domain performance simulation as a hybrid offering on its cloud platform. With this offering, users can harness the power of Virtual Performance Solution, leading multi-domain CAE solution for virtual engineering of crash, safety, comfort, NVH (noise, vibration and harshness), acoustics, stiffness and durability.

In this hybrid model, users utilize VPS on their desktop for modeling including geometry, meshing and simulation set up. ESI Cloud is then used for high performance computing with an integrated visualization and real time collaboration offering through a web browser.

The benefits of VPS hybrid on ESI Cloud include:

- Running large concurrent simulations on demand
- On demand access to scalable and secured cloud HPC resources
- Three tiered security strategy for your data
- Visualization of large simulation data sets
- Real-time browser based visualization and collaboration
- Time and cost reduction for data transfer between cloud and desktop environments
- Support, consulting and training services with ESI's engineering teams

VPS On Demand

ESI Cloud features the Virtual Performance Solution (VPS) enabling engineers to analyze and test products, components, parts or material used in different engineering domains including crash and high velocity impact, occupant safety, NVH and interior acoustics, static and dynamic load cases. The solution enables VPS users to overcome hardware limitations and to drastically reduce their simulation time by running on demand very large concurrent simulations that take advantage of the flexible nature of cloud computing.

Key solution capabilities:

- Access to various physics for multi-domain optimization
- Flexible hybrid model from desktop to cloud computing
- On demand provisioning of hardware resources
- Distributed parallel processing using MPI (Message Passing Interface) protocol
- Distributed parallel computing with 10 Gb/s high speed interconnects

Result visualization

ESI Cloud deploys both client-side and server-side rendering technologies. This enables the full interactivity needed during the simulation workflow along with the ability to handle large data generated for 3D result visualization in the browser, removing the need for time consuming data transfers. Additionally ESI Cloud visualization engine enables the comparisons of different results through a multiple window user interface design.

Key result visualization capabilities:

- CPU or GPU based client and server side rendering
- Mobility with desktop like performance through the browser
- 2D/3D VPS contour plots and animations
- Custom multi-window system for 2D plots and 3D contours
- Zooming, panning, rotating, and sectioning of multiple windows

Collaboration

To enable real time multi-user and multi company collaboration, ESI Cloud offers extensive synchronous and asynchronous collaboration capabilities. Several users can view the same project, interact with the same model results, pass control from one to another. Any markups, discussions or annotations can be archived for future reference or be assigned as tasks to other members of the team.

Key collaboration capabilities:

- Data, workflow or project asynchronous collaboration
- Multi-user, browser based collaboration for CAD, geometry, mesh and results models
- Real-time design review with notes, annotations and images archiving and retrieval
- Email invite to non ESI Cloud users for real time collaboration

TOYOTA - Total Human Model for Safety – THUMS

The Total Human Model for Safety, or THUMS®, is a joint development of Toyota Motor Corporation and Toyota Central R&D Labs. Unlike dummy models, which are simplified representation of humans, THUMS represents actual humans in detail, including the outer shape, but also bones, muscles, ligaments, tendons, and internal organs. Therefore, THUMS can be used in automotive crash simulations to identify safety problems and find their solutions.

Each of the different sized models is available as sitting model to represent vehicle occupants

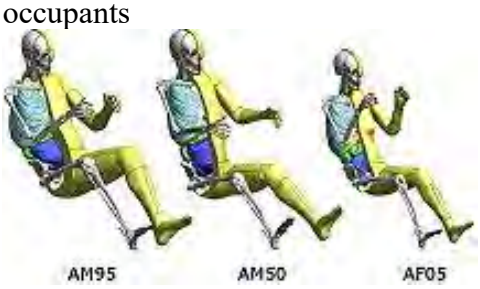

and as standing model to represent pedestrians.

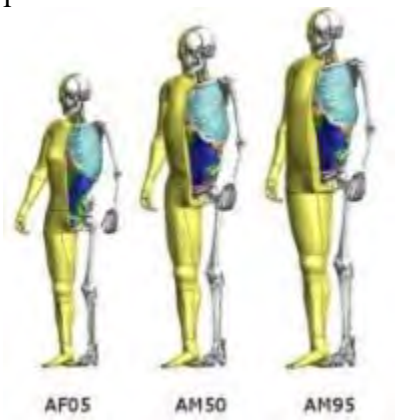

The internal organs were modeled based on high resolution CT-scans.

THUMS is limited to civilian use and may under no circumstances be used in military applications.

LSTC is the US distributor for THUMS. Commercial and academic licenses are available.

For information please contact: THUMS@lstc.com

THUMS®, is a registered trademark of Toyota Central R&D Labs.

LST, An ANSYS Company – Dummy Models

Crash Test Dummies (ATD)

Meeting the need of their LS-DYNA users for an affordable crash test dummy (ATD), LSTC offers the LSTC developed dummies at no cost to LS-DYNA users.

LSTC continues development on the LSTC Dummy models with the help and support of their customers. Some of the models are joint developments with their partners.

e-mail to: atds@lstc.com

Models completed and available (in at least an alpha version)

- Hybrid III Rigid-FE Adults
- Hybrid III 50th percentile FAST
- Hybrid III 5th percentile detailed
- Hybrid III 50th percentile detailed
- Hybrid III 50th percentile standing
- EuroSID 2
- EuroSID 2re
- SID-IIs Revision D
- USSID
- Free Motion Headform
- Pedestrian Legform Impactors

Models In Development

- Hybrid III 95th percentile detailed
- Hybrid III 3-year-old
- Hybrid II
- WorldSID 50th percentile
- THOR NT FAST
- Ejection Mitigation Headform

Planned Models

- FAA Hybrid III
- FAST version of THOR NT
- FAST version of EuroSID 2
- FAST version of EuroSID 2re
- Pedestrian Headforms
- Q-Series Child Dummies
- FLEX-PLI

LST, An ANSYS Company – Barrier Models

Meeting the need of their LS-DYNA users for affordable barrier models, LSTC offers the LSTC developed barrier models at no cost to LS-DYNA users.

LSTC offers several Offset Deformable Barrier (ODB) and Movable Deformable Barrier (MDB) models:

- ODB modeled with shell elements
- ODB modeled with solid elements
- ODB modeled with a combination of shell and solid elements
- MDB according to FMVSS 214 modeled with shell elements
- MDB according to FMVSS 214 modeled with solid elements
- MDB according to ECE R-95 modeled with shell elements
- AE-MDB modeled with shell elements
- IIHS MDB modeled with shell elements
- IIHS MDB modeled with solid elements
- RCAR bumper barrier
- RMDB modeled with shell and solid elements

LSTC ODB and MDB models are developed to correlate to several tests provided by our customers. These tests are proprietary data and are not currently available to the public.

All current models can be obtained through our webpage in the LSTC Models download section or through your LS-DYNA distributor.

To submit questions, suggestions, or feedback about LSTC's models, please send an e-mail to: atds@lstc.com. Also, please contact us if you would like to help improve these models by sharing test data.

Social Media

FACEBOOK

BETA CAE Systems
CADFEM
ESI Group

TWITTER

BETA CAE Systems
ESI Group
ETA
CADFEM

LINKEDIN

BETA CAE Systems
CADFEM
DYNAmore Nordic
ETA
ESI Group

YOUTUBE

YOUTUBE Channel	WebSite URL
BETA CAE Systems	www.beta-cae.com
CADFEM	www.cadfem.de
ESI Group	www.esi-group.com
ETA	www.eta.com
Lancemore	www.lancemore.jp/index_en.html
LS-DYNA OnLine - (Al Tabiei)	https://www.youtube.com/user/LSDYNATV

GOOGLE+

BETA CAE Systems